GTI/DOE/SMP/GRI-61134/80042/30797

Final Technical Report

Laboratory Development of a High Capacity Gas-Fired Paper Dryer

Prepared by:

Gas Technology Institute

Gas Technology Institute

Energy Utilization Center
September 2004

GTI/DOE/SMP/GRI-61134/80042/30797

Laboratory Development of a High Capacity Gas-Fired Paper Dryer

FINAL TECHNICAL REPORT
(February 2001 to June 2004)

Prepared by

Yaroslav Chudnovsky, Ph.D.
Aleksander Kozlov, Sc.D.
Lester Sherrow, M.S.

Energy Utilization Center/Process Heating
Gas Technology Institute
1700 S. Mount Prospect Rd.
Des Plaines, IL 60018

Prepared for:

US Department of Energy/Industrial Technology Programs

Dixon Ozokwelu, Ph.D., P.E., Joseph Springer, PMP

GTI Sustaining Membership Program

Ron Snedic

Gas Research Institute

Hamid Abbasi

September 2004

LEGAL NOTICE

This report was prepared by the Gas Technology Institute ("GTI") as an account of work sponsored by the US Department of Energy (DOE ITP), GTI's Sustaining Membership Program (SMP), and Gas Research Institute (GRI). Neither DOE ITP, SMP, GRI, nor their members, nor any party acting on behalf of any of them:

a. makes any warranty or representation, express or implied, with respect to the accuracy, completeness, or usefulness of the information contained in this report, or that the use of any apparatus, method, or process disclosed in this report may not infringe privately owned rights; or

b. assumes any liability with respect to the use of, or for damages resulting from the use of, any information, apparatus, method, or process disclosed in this report.

REPORT DOCUMENTATION PAGE

Form Approved
OMB No. 0704-0188

1. AGENCY USE ONLY (*Leave blank)*	2. REPORT DATE	3. REPORT TYPE AND DATES COVERED
	September 2004	Final Technical Report (March 2001- June 2004)

4. TITLE AND SUBTITLE

Laboratory Development of a High Capacity Gas-Fired Paper Dryer

5. FUNDING NUMBERS

DOE: DE-FC36-01GO10621
GRI: Contract 8477

6. AUTHOR(S)

Yaroslav Chudnovsky, Aleksandr Kozlov, Lester Sherrow

7. PERFORMING ORGANIZATION NAME(S) AND ADDRESS(ES)

Gas Technology Institute
1700 S. Mount Prospect Rd.
Des Plaines, IL 60018

8. PERFORMING ORGANIZATION REPORT NUMBER

15320.1.01
15401.1.01
15058.4.06

9. SPONSORING/MONITORING AGENCY NAME(S) AND ADDRESS(ES)

Department of Energy, 1000 Independence Avenue, SW, Washington, DC 20585
Sustaining Membership Program, 1700 South Mount Prospect Road, Des Plaines, IL 60018
Gas Research Institute, 1700 South Mount Prospect Road, Des Plaines, IL 60018

10. SPONSORING/MONITORING AGENCY REPORT NUMBER

11. SUPPLEMENTARY NOTES

12a. DISTRIBUTION/AVAILABILITY STATEMENT

12b. DISTRIBUTION CODE

13. ABSTRACT (*Maximum 200 words)*

Paper drying is the most energy-intensive and temperature-critical aspect of papermaking. It is estimated that about 67% of the total energy required in papermaking is used to dry paper. The conventional drying method uses a series of steam-heated metal cylinders that are required to meet ASME codes for pressure vessels, which limits the steam pressure to about 160 psig. Consequently, the shell temperature and the drying capacity are also limited.

Gas Technology Institute together with Boise Paper Solutions, Groupe Laparrier and Verreault (GL&V) USA Inc., Flynn Burner Corporation and with funding support from the U.S. Department of Energy, U.S. natural gas industry, and Gas Research Institute is developing a high efficiency gas-fired paper dryer based on a combination of a ribbon burner and advanced heat transfer enhancement technique. The Gas-Fired Paper Dryer (GFPD) is a high-efficiency alternative to conventional steam-heated drying drums that typically operate at surface temperatures in the 300ºF range.

The new approach was evaluated in laboratory and pilot-scale testing at the Western Michigan University Paper Pilot Plant. Drum surface temperatures of more than 400ºF were reached with linerboard (basis weight 126 lb/3000 ft^2) production and resulted in a 4-5 times increase in drying rate over a conventional steam-heated drying drum. Successful GFPD development and commercialization will provide large energy savings to the paper industry and increase paper production rates from dryer-limited (space- or steam-limited) paper machines by an estimated 10 to 20%, resulting in significant capital costs savings for both retrofits and new capacity.

14. SUBJECT TERMS	15. NUMBER OF PAGES
	16. PRICE CODE

17. SECURITY CLASSIFICATION OF REPORT	18. SECURITY CLASSIFICATION OF THIS PAGE	19. SECURITY CLASSIFICATION OF ABSTRACT	20. LIMITATION OF ABSTRACT
Unclassified	Unclassified	Unclassified	

Contents

EXECUTIVE SUMMARY

Paper drying consumes about 67% of the total energy required in papermaking, and the production capacity of papermaking plants is often limited by dryer capacity. Conventional paper drying passes the wet paper web over a series of metal drums that are internally heated by condensing steam. Pressure vessel codes limit the steam pressure to 160 psi and, therefore, the steam temperature to about 370ºF. This project investigated the feasibility of using drums that are heated by burning natural gas inside them. These drums could operate at higher temperature, increasing energy efficiency and improving production capacity.

The technical concept on which the project was based was to enhance heat transfer and combustion stability by putting large dimples in the internal surface of the drums. Two concepts were investigated in the laboratory, one with combustion taking place inside the dimples, and one with the combustion outside the dimples. The latter approach was found to be better, and it led to the design and testing of a prototype gas-fired paper-dryer (GFPD) drum. The drum's performance was tested in GTI's combustion laboratory and in a small-scale paper-drying pilot plant at Western Michigan University.

The results showed significant increases in drying speed and efficiency. Development of a larger GFPD and testing in a larger-scale paper drying line is recommended. This further development should:

1. Determine the optimum number and position of GFPD drums in a paper line.
2. Verify adequate temperature uniformity across the drum to maintain paper quality.
3. Further improve GFPD efficiency.
4. Reduce NO_x emissions to 20-30 ppm.
5. Ensure safe operation.

Successful development of the GFPD will help the paper industry increase production of dryer-limited paper machines by 10 to 20%, resulting in significant capital savings for both retrofits and new capacity. A corresponding energy efficiency increase from 65% to over 80% will provide large energy savings. Assuming 86 million tons/year of paper and paperboard products and 2,000 Btus needed to evaporate 2 pounds of water per pound of dried paper, the proposed approach, if retrofit to only 5% of the steam drums now in use, would save an estimated 5 trillion Btu's of fuel and 700 tons of NO_x emissions annually, compared to conventional steam drums. Although the payback period will be site-specific, it is estimated to be less than 1 year.

PROJECT SUMMARY

Overall Project Objective

The primary objective of this project was to provide experimental confirmation of the technical and economic feasibility of an innovative, low cost, natural gas-fired cylinder paper dryer, which would be suitable for both retrofit and new installations.

Rationale for Undertaking the Project

Conventional paper drying uses a series of metal drums that are internally heated by condensing steam. The use of steam requires the drums to meet ASME codes for pressure vessels, which limits the steam pressure to 160 psi and, therefore, the steam temperature to about 370ºF, and the drum surface temperatures are, of course, even lower. Paper drying is the most energy-intensive and temperature-critical aspect of papermaking (about 67% of the total energy required in papermaking). Paper machine speeds, and therefore production rates, are frequently limited by dryer capacity. A great deal of activity has therefore been devoted to developing new, high efficiency, high rate paper drying equipment (gas-fired alternatives were developed by British Gas - Patent Application WO 99/45196, ABB Drying - US Patent 5,791,065, Gastec NV - US Patent 5,842,285, but only ABB was able to introduce its design to the commercial market). GTI initiated developing an innovative approach to natural gas-fired combustion systems that can significantly improve paper drying efficiency, decrease specific energy consumption, and overcome the limitations of pre-mixing while still producing stabilized combustion. The approach involves a successful combination of low-NO_X natural gas combustion and an advanced heat transfer enhancement technique.

Brief Description of Project

The project consisted of two phases:

Concept Feasibility Study (Phase I) – Year One. Two major concepts were evaluated– Flame-Inside-Dimple (FID) and Flame-Outside-Dimple (FOD). These two concepts were tested on a bench-scale unit (up to 85,000 Btu/hr) in GTI's applied combustion research laboratory, using stationary dimpled elements. This testing was partially based on internally funded proof-of-concept work initiated at GTI.

Development Testing (Phase II) - Year Two. The resulting data from the first phase was used to design a pilot-scale (up to 150,000 Btu/h) gas-fired dryer drum, which was tested at GTI Applied Research Laboratory for combustion performance and then was installed in a pilot-scale paper machine located at the Western Michigan University Paper Pilot Plant. GTI, along with industrial partners (Flynn Burner Co., GL&V USA Inc. and Boise Paper Solutions) evaluated the performance of the pilot-scale paper dryer under near-industrial conditions for drum temperature level and uniformity, heat transfer rates, emission levels, and energy efficiency.

This report describes both phases of the project.

As illustrated in Figure 1, the FID approach involved combusting natural gas with air in hemispherical dimples. Natural gas was injected inside the dimple, while combustion air was

supplied from the outside. Figure 1a shows how the flow of combustion air generated a vortex in the dimple, which resulted in good mixing of natural gas and air and stabilized the combustion process. Each fired dimple formed its own flame, as shown in the photograph in Figure 1b, which interacted with the flames from other cavities, forming the vortex flame pattern. Preliminary tests[1] have shown that combustion is stable over a wide range of air velocities.

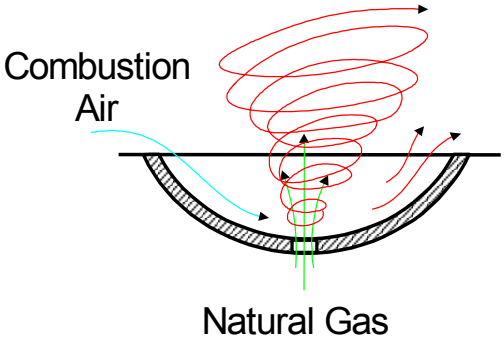

Figure 1a. Vortex Formed By Combustion Air Flow Results In Intense Gas-Air Mixing

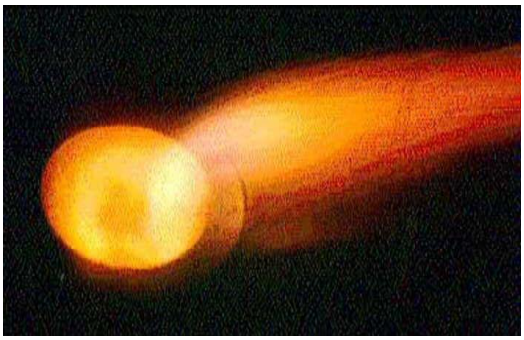

Figure 1b. A Highly Stable Flame Is Formed Within Each Dimple

In the FOD approach, the flame sheet extends over the dimpled surface in an annular space inside the drum to provide low-emission recirculation flow and a high heat transfer rate from the combustion zone to the drying drum (Figure 2).

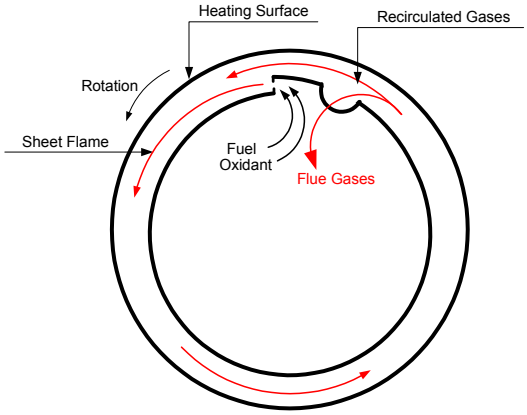

Figure 2. Concept and Flame Image of the FOD Approach

After completing laboratory bench-scale evaluation of the above two concepts, the FOD concept was selected for further development and testing in Phase 2. A gas-fired paper dryer (GFPD) prototype, based on the FOD concept, was developed, built, and tested. The concept

[1] Ya. Chudnovsky, A. Kozlov et al., "Combustion Enhancement and Flame Stabilization Due to Vortex Generation." Proc. 1997 AFRC International Symposium: *Combustion Technology for Improving Productivity and Product Quality*, Chicago, IL, September 21-24, 1997.

was finalized, as represented in Figure 2. A U.S. patent application (10/454,021) has been submitted.

Project Work Scope

Phase I: Concept Feasibility Study

Task 1. Bench-scale unit (BSU) design	– completed
Task 2. BSU fabrication	– completed
Task 3. BSU laboratory testing	– completed
Task 4. Data processing/analysis	– completed
Task 5. Technical report on Phase I	– completed

Phase II: Development Testing

Task 6. Design of pilot-scale unit	– completed
Task 7. Fabrication of pilot-scale unit	– completed
Task 8. Laboratory testing of pilot-scale unit at GTI	– completed
Task 9. Pilot-scale testing at WMU's pilot-scale paper machine	– completed
Task 10. Data processing and analysis	– completed
Task 11. Technical report on Phase II /Final	– completed

CONCEPT FEASIBILITY STUDY (Phase I)

FID Concept Evaluation

A bench-scale unit (BSU) was designed, fabricated, and assembled (including air/gas supply unit, gas distribution system, wheeled-base, flex-chimney and set of dimpled test elements). A measurement system was developed and installed.

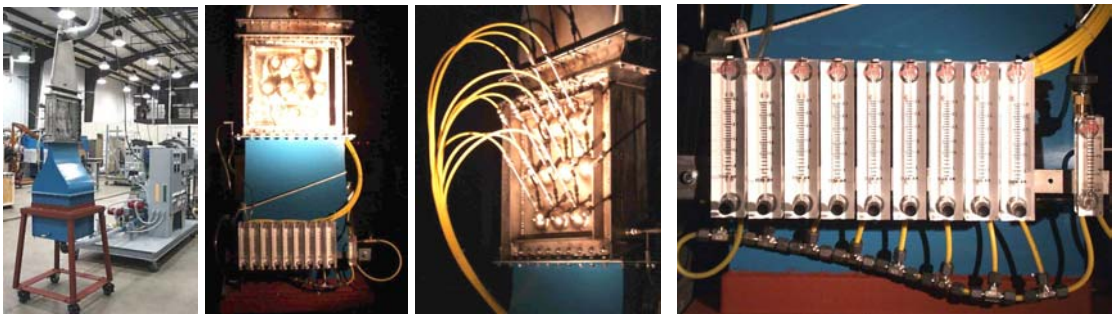

General views Gas Injectors Gas Rotameters

Figure 3. BSU for FID Concept Evaluation

The assembled system allowed visual observation and registration of the combustion flow pattern as well as measuring the following parameters:

- air and gas flow rates
- inlet air flow velocity profiles
- inlet and outlet flow temperature
- wall temperature
- composition of the combustion products

Five square test plates with varying dimple size and density were designed and fabricated (see Figures 4 and 5 and Table 1). All the test plates were reinforced with an angled frame to prevent thermal distortion.

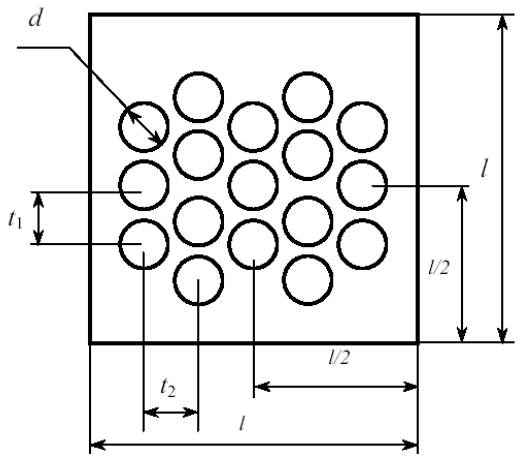

Figure 4. Geometry of Dimpled Profile

Table 1. Geometry of Dimpled Profile

Dimple plate No.	Dimple diameter d, in	t_1, in	t_2, in	Dimple relative density, $f=\pi d^2/(t_1 t_2 2\sqrt{3})$	Side size l, in	Comments *
1	1.25	2.625	2.25	0.24	14	17 dimples, 5 rows 17 gas nozzles
2	1.25	2.625	2.25	0.24	14	17 dimples, 5 rows 17 gas nozzles, extension
3	2.0	2.625	2.25	0.61	14	17 dimples, 5 rows 17 gas nozzles
4	2.0	2.625	2.25	0.61	14	17 dimples, 5 rows 17 gas nozzles, extension
5	2.0	3.0	4.5	0.27	14	10 dimples, 3 rows 20 gas nozzles

* *All dimples were hemispherical*

Test plates were installed one by one into the back side of a test section frame. A high-temperature fused quartz glass served as the front side of the test section to provide visualization capability.

Plate # 3 after welding

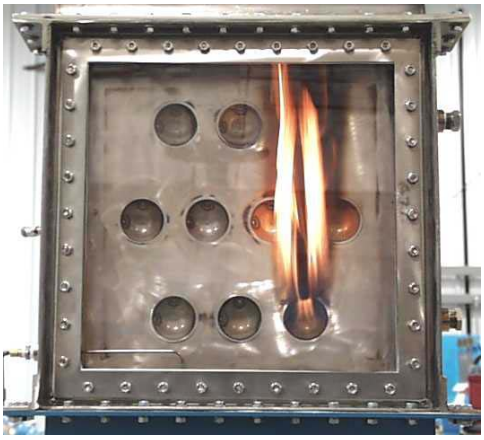

Plate # 5 installed in the BSU test section

Rear view of dimpled plates #3 and #5 with gas injectors installed

Figure 5. Views of Dimpled Plates

BSU shakedown was conducted. Combustion flow structure (Figure 6) and operational characteristics of the bench-scale unit were also estimated:

- incoming air flow velocity range: 0-15 ft/s (1.5″ gap) and 0-60 ft/s (0.375″ gap)
- air flow rate through a nozzle: 0-100 SCFH
- gas flow rate through a nozzle: 0-40 SCFH
- overall pressure drop: up to 25” WC at the highest air flow rate
- inlet flow velocity profile is uniform in whole flow velocity range (the non-uniformity profile is less than 5% of mean velocity)

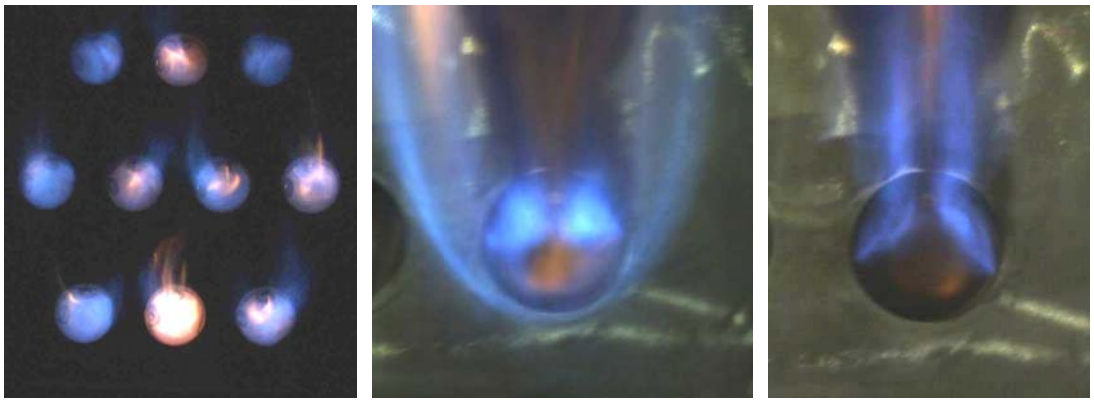

Figure 6. Flame Structures During Shakedown Firing

Smoke flow visualization (with no combustion) inside a dimple for two dimple diameters, two channel heights, and 5 dimpled plates at different incoming air flow velocities confirmed the results of a prior study of the vortex pattern inside the dimples. Repetitive combustion tests with various dimple arrangements showed that incoming air and gas flow rates ratios, gas nozzle positions and geometries, and various obstacles affected combustion stability. The following factors were the most effective in stabilizing combustion inside the dimple:

- gas injector geometry and position;
- obstacle installed upstream or downstream of the dimple

Gas injector optimal position and geometry were determined for the purpose of stable combustion inside the dimple. The gas injector with optimal geometry had a hole on the tube side, so the gas (or mixture) jet was injected along the dimple wall (Figure 7).

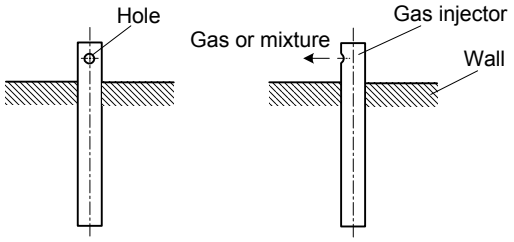

Figure 7. Optimal Geometry of the Gas Injector

Several gas injector positions gave stable combustion inside the dimple. Some of them are shown in plan view in Figure 8.

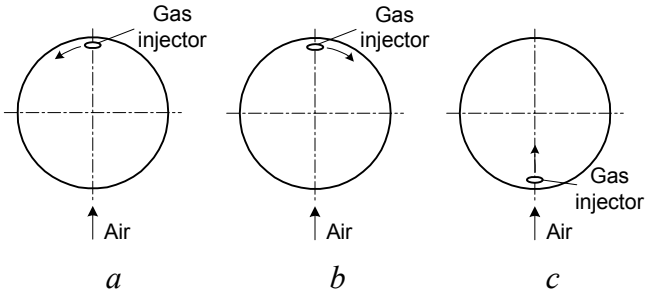

Figure 8. Optimal Positions of the Gas Injector for Stable Combustion

A small obstacle in the form of a round rod installed upstream of the dimple improved combustion stability, while a flat plate installed in the upstream part of the dimple (Figure 9) inhibited flame propagation completely.

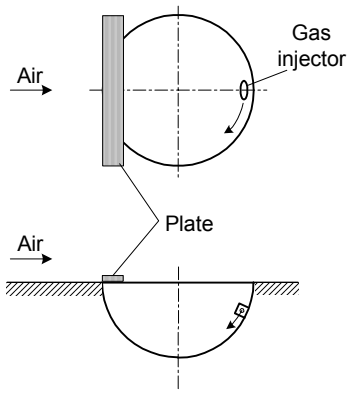

Figure 9. Plate Installed Upstream of the Dimple Kills The Flame

Repetitive tests for the purpose of achieving complete combustion inside the dimple (as well as in the dimple arrangement) showed that the incoming air and gas flow rates ratio, gas nozzle positions and geometries, and premixing of the air/gas mixture affected completeness of combustion. Combustion flow patterns inside the dimple depended on the incoming air and gas flow rates ratio:

- The flame inside a dimple is exposed to buoyancy effects and doesn't follow the air flow (Figure 10a) when the incoming air flow velocity is too low (for instance, less than 10 ft/s when gas flow rate is more than 1 SCFH). In this case, the dimple doesn't properly stabilize the flame or organize combustion on the dimpled surface. The emissions are not controllable by the dimple and are the same as for a regular diffusion flame in an air flow.
- The combustion flow pattern inside the dimple is formed by the injected gas jet (Figure 10b) when the gas flow rate through the injector is too high (for instance, higher than 2 SCFH when incoming air flow velocity is less than 10 ft/s). This situation is not favorable for combustion either, as a large amount of unburned gas is ejected from the dimple into the incoming air flow, causing incomplete combustion.

– There are combustion flow regimes when the flame inside the dimple is formed by self-organized vortex flow caused by the incoming air flow (Figure 10c). This is the most desirable situation for having complete combustion in the dimple because it gives higher residence time for the air/gas mixture inside the dimple.

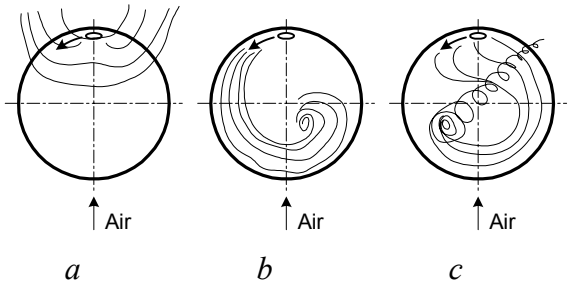

Figure 10. Combustion Flow Pattern Inside the Dimple at Different Air/Gas Flow Rates Ratios

Very high levels of oxygen (up to 20%), carbon monoxide (up to 1000 vppm), and total hydrocarbon (up to 3000 vppm) were registered in the exhaust gas downstream from the dimple (Figures8a and 8b). Having the gas injector in the upstream position (Figure 8c) led to a more complete combustion (5-15 vppm of total hydrocarbon at 19-20% of oxygen in the exhaust gas). However, there is a limitation on firing rates that achieve complete combustion. There was complete combustion at low gas flow rates only when the flame was entirely inside the dimple. If the flame was out of the dimple, combustion was incomplete. It was possible to improve the completeness of combustion in the dimple at high firing rate by injecting additional air flow from adjacent dimples or the upstream dimples.

Partial and complete premix inside the dimple was tested for its effect on completeness of combustion. Premixed air and gas was injected through the gas injector. The tests demonstrated that only full premix and a high firing rate (more than 6 SCFH of gas flow rate for 2-inch diameter dimples) provided complete combustion. Total hydrocarbon content decreased to a few vppm when the dimple wall has heated up to 600-700ºF).

Based on the data obtained for a single dimple, tests for the dimple arrangement were carried out. The objective of these tests with premixed air and gas was to prove the viability of complete combustion in a dimple with perfect mixing. It was decided that, since complete combustion was attained for one row of dimples, there was no need to fire the entire dimpled plate and risk an anticipated high heat release that could have damaged the elements of the test section.

A non-premix approach with the gas injector in the upstream position of the dimple (Figure 8c) for the dimple arrangement did not provide complete combustion, just as in the case of one dimple. In the dimple arrangement, the dimples had an influence on each other, increasing or decreasing (depending on the dimple arrangement) combustion stability.

It was also attempted to study combustion for two rows of dimples (Figure 11): the first row (3 dimples) with non-premix and the second row (4 dimples) with premix. The purpose of the experiment was to test whether unburned hydrocarbons from the first row of the dimples would burn in the second row of the dimples. The experiments showed that complete combustion after second row of the dimples was not achieved.

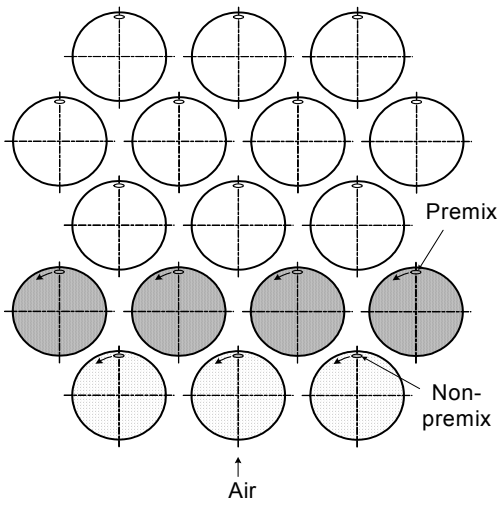

Figure 11. Dimple Arrangement With Non-Premix (1st Row of the Dimples) and Premix (2nd Row of the Dimples) Combustion

In order to look deeper in the nature of vortex combustion structure, experiments were conducted with a single dimple at minimal excess air. For these experiments, the height and width of the test channel were narrowed, as shown in Figure 12. The new channel geometry allowed us to eliminate or decrease the influence of such factors as surrounding dimples and excess air.

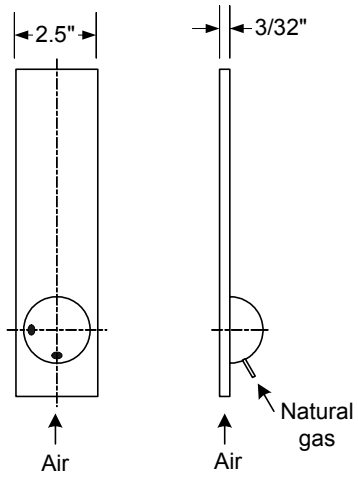

Figure 12. A Single Dimple in the Narrow Channel

Experimental conditions and testing results for the FID concept evaluations are presented below.

Flow rates:

Air ~ 24-200 SCFH (velocity – 1-10.5 m/s)

Natural gas ~ 2-10 SCFH

Natural gas nozzle geometry:

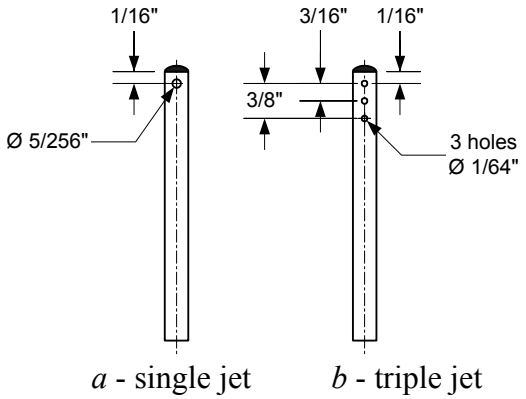

Natural gas jet direction

Five different natural gas injection directions were tried (see Figure 13*a-d* – gas injected near the surface, and *e* – gas injected from the dimple center)

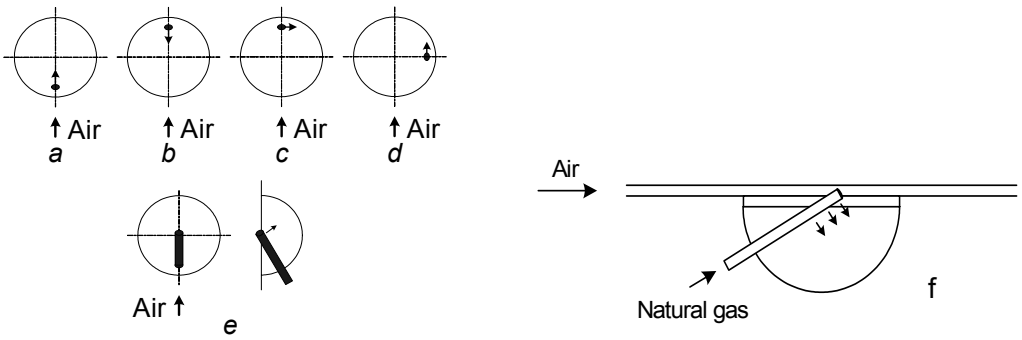

Figure 13. Directions of Natural Gas Injection

In most cases, it was not possible to achieve less than 10% oxygen in the exhaust gas.

The most complete combustion was achieved for dimpled plate No. 4, which had deep dimples (hemispherical dimples with a cylindrical ring), using a 3-hole natural gas nozzle installed downstream inside the dimple (see Figure 13f). In this case, there was 4% oxygen in the exhaust gas at an air flow rate of 70 SCFH and a natural gas flow rate of 6 SCFH. Total hydrocarbon concentration was 2000-5000 ppm. CO concentration was about 2500 ppm. Variants of combustion patterns for configuration f are shown in Figure 14. For the other configurations, the concentration of total hydrocarbons was more than 5000 ppm.

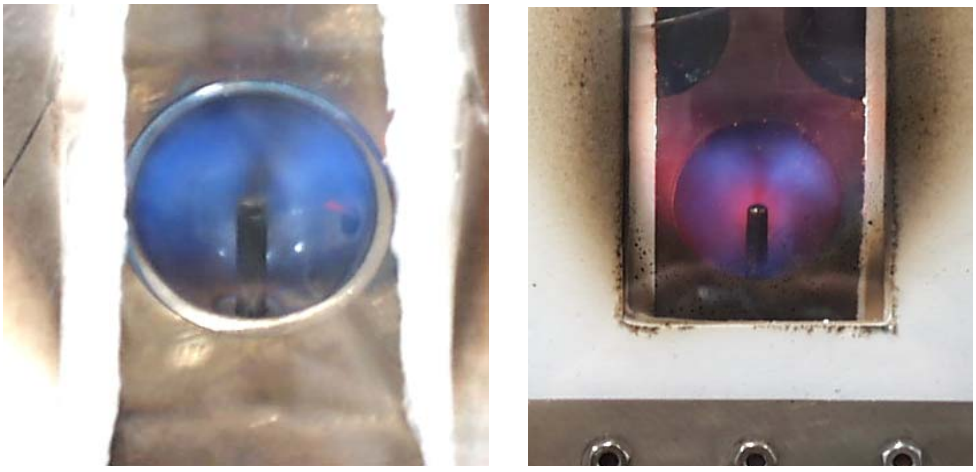

COLD START STEADY OPERATION

Figure 14. Combustion Pattern Within a Single Dimple with a 3-Hole Natural Gas Nozzle

Dimple Depth

In order to retain the combustion vortex inside the dimple (to provide complete combustion), one of the front dimples on dimple plate No. 3 was reworked by increasing the dimple depth (Figure 15). The dimple depth was changed from 1" to 2". Channel height in those experiments was ~ 0.1".

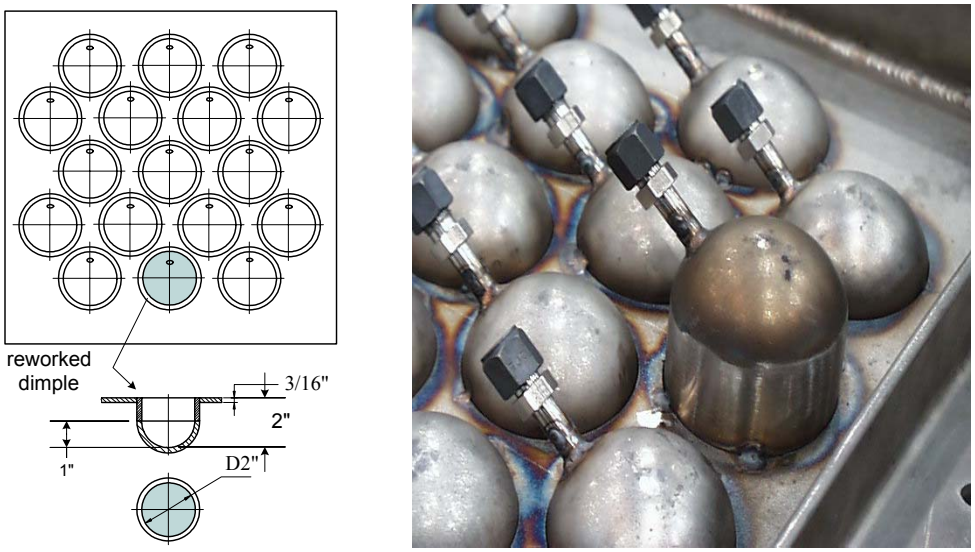

Figure 15. Dimple Plate No. 3 (Staggered Arrangement of the Hemispherical Dimples With 2" Diameter) With a Dimple of 2" Depth

The following results were obtained in the course of the experiments with a deep dimple:

- It was difficult to ignite natural gas at air velocities < 10 ft/s. The flame was unstable, and no instance of complete combustion was observed. It even was impossible to ignite the gas at some configurations of the dimple and gas nozzle.

- There was stable and complete combustion inside the deep dimple at air velocities > 10 ft/s and gas flow rates < 1 SCFH. In these cases, the flame was sitting inside the dimple. Typical exhaust composition was: O_2 < 20.5%, CO ~ 1 ppm, CO_2 ~ 0%, THC < 5 ppm, and NO_x < 1 ppm
- Stable and complete combustion could not be achieved at gas flow rates > 1 SCFH. In these cases, the flame detached from the dimple.

Dual Fuel Nozzles

The next step in pursuing complete combustion inside the dimple was to incorporate a dual-nozzle approach. One nozzle was used for air injection, another for gas injection (Figure 16). Channel height was ~ 0.1".

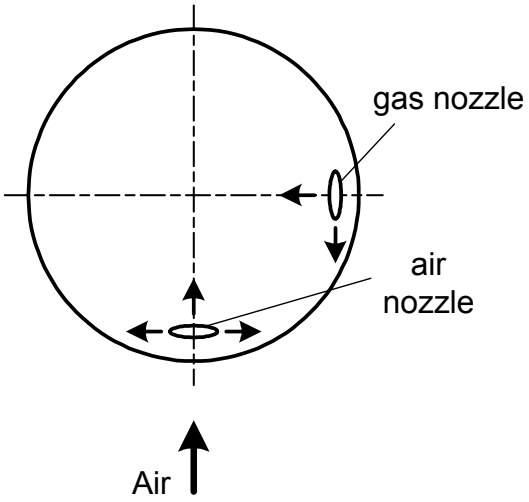

Figure 16. Dual-Nozzle Approach

Incoming air velocity was 3-30 ft/s. Air flow rate through the nozzle was 1-100 SCFH. Gas flow rate was 0.5-10 SCFH. Experiments showed that the flame was not stable enough, i.e., the flame vortex remained outside of the dimple, and overall combustion was not complete.

Dimple Shape

A series of combustion experiments was conducted by using high-temperature foil inside and outside the dimple to form specific flow structures. Aluminum foil (~ 0.1 mm thickness) was used to reshape the dimple surface and determine the degree of the dimple shape influence on the combustion structure inside the dimple. Some of the dimple shapes and gas nozzle positions are shown in Figure 17.

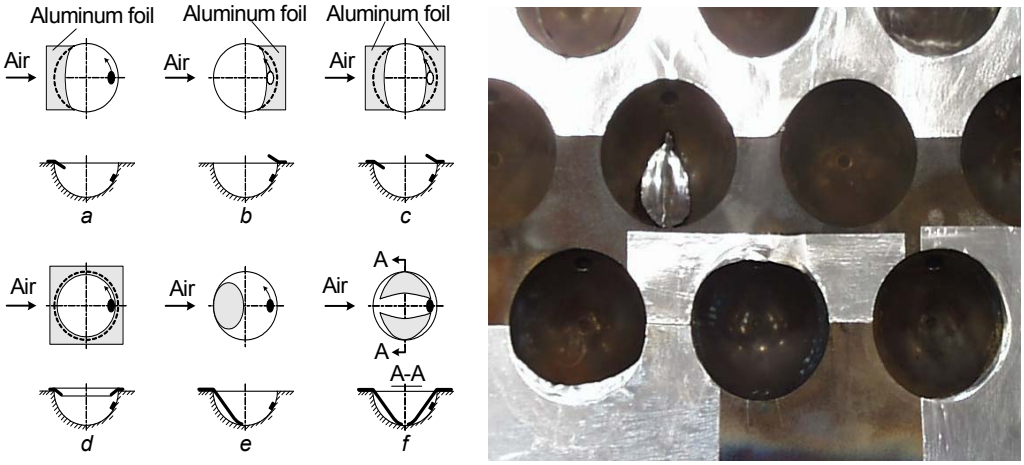

Figure 17. Dimples Shaped by Aluminum Foil

These experiments established that the dimple shape influences flame stability and combustion completeness very much. But complete combustion was not achieved for all investigated configurations (THC > 5-10% at O_2 > 18%).

Combustion Between Two Dimpled Walls

Combustion inside a narrow duct between two dimpled walls (Figure 18) was studied, and exhaust composition was measured. In these experiments, both test section walls were dimpled (the quartz glass was replaced by a dimpled plate).

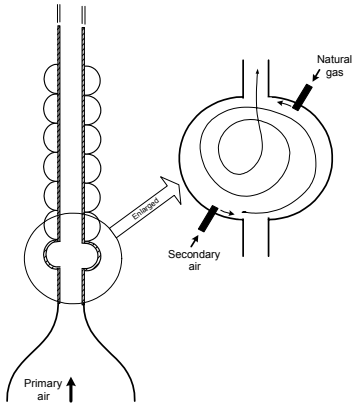

Figure 18. Test Channel Formed by Two Opposing Dimpled Plates

Experimental conditions:

- Distance between the walls was 0.375”
- Primary air velocity was 3-30 ft/s.
- Secondary air flow rate was 0-100 SCFH
- Natural gas flow rate was 2-10 SCFH

Since it was quite difficult to ignite natural gas blindly with no glass wall or peep hole, the flame structure was not observed and registered. In the best case, 8-10 ppm of THC (practically unburned natural gas) was measured at ~ 19.5% O_2, primary air velocity ~ 1.5-2.0 ft/s, and natural gas flow rate of 2 SCFH, with no secondary air flow.

Natural Gas Injection Over the Dimpled Plate

A linear flame approach, similar to one used in jet engines, was tested for its ability to achieve complete combustion on the dimpled plate. A tubular gas distributor with holes was used as a burner inside a narrow duct with a dimpled wall (Figure 19). The experiments were performed in order to check the idea of using natural gas afterburning.

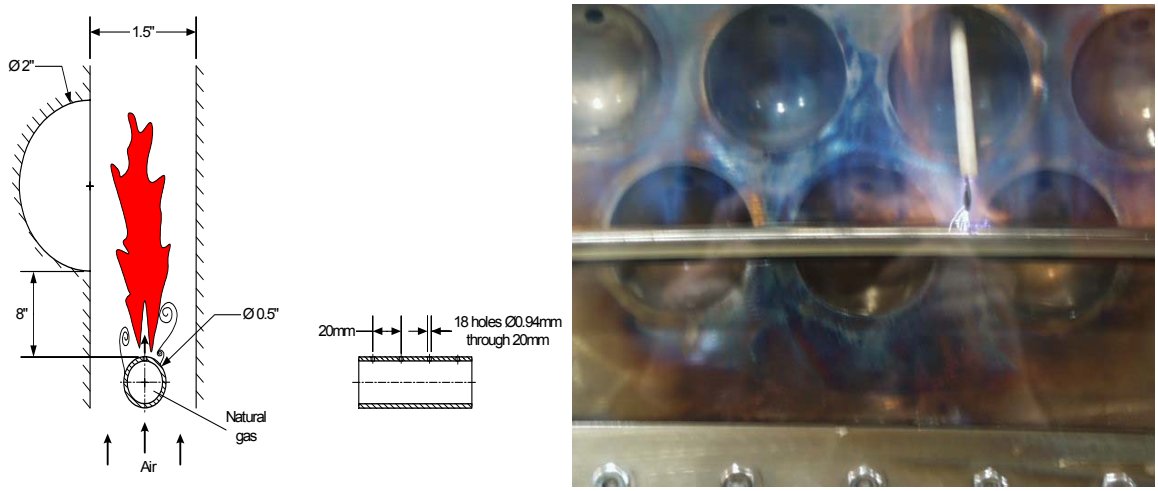

Figure 19. Tubular Gas Distributor Inside a Narrow Duct With a Dimpled Wall

Experimental conditions:

- Air velocity was 16-65 ft/sec.
- Natural gas total flow rate was 10-100 SCFH

Exhaust gas composition for the best case was: O_2 – 20.4%, CO_2 ~ 0.1%, CO – ~ 110 ppm, THC – 100 ppm (~ 4% unburned methane), NO_x - ~ 2 ppm at air velocities of about 45 ft/s and natural gas flow rate of 40 SCFH.

There was a very unstable flame at high natural gas flow rates (> 50 SCFH). Pressure drop at the duct was 0.26" WC. Complete combustion could not be achieved at any tested flow velocity and gas flow rate.

Wing Stabilizers

The idea of using a gas nozzle with wing stabilizers (Figure 20) to increase the amount of air injected into the gas flow was also tested.

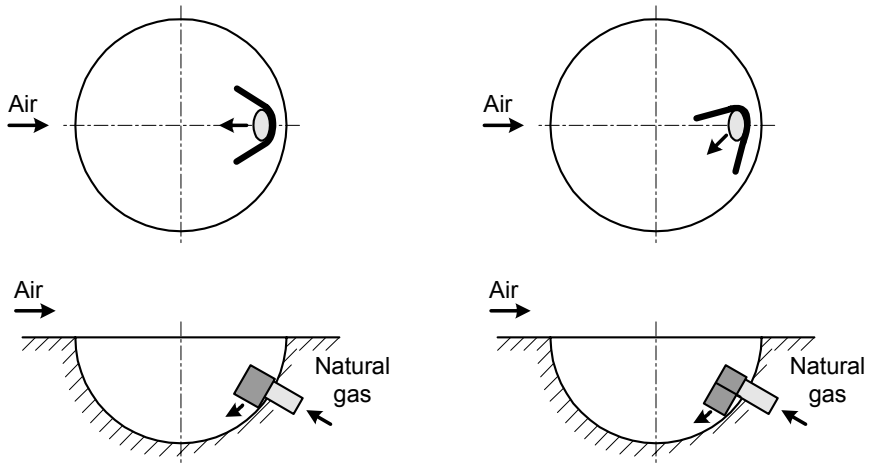

Figure 20. Gas Nozzle With a Wing Stabilizer

Experimental conditions:

- Channel height was 1.5 inches
- Air flow velocity was 15-30 ft/s
- Natural gas flow rate was 1-10 SCFH

Exhaust gas composition for the best case was: O_2 – 20.7%, CO – 7 ppm, CO_2 – 0.0%, THC – 7 ppm, NO_x – 0.2 ppm at an air velocity of ~ 30 ft/s and a gas flow rate of 2.5 SCFH per dimple.

During the testing, more stable combustion was observed with the stabilizer than without it. A higher firing rate was also achieved with the stabilizer. Incomplete combustion (unburned methane) was registered at gas flow rates exceeding 6 SCFH.

Higher Air Injection

The idea of increasing the amount of air injected into the gas flow was experimentally checked, as shown in Figure 21.

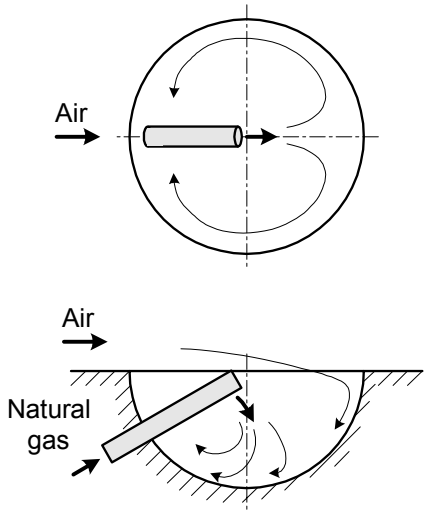

Figure 21. Extended Gas Nozzle Introduced in Flow

Experimental conditions:

- Channel height was 1.5 inches
- Air flow velocity was 15-30 ft/s
- Natural gas flow rate was 0.6-5 SCFH

The exhaust gas composition for the best case was: O_2 – 20.7%, CO – 12 ppm, CO_2 – 0.0%, THC – 24 ppm, NOx – 0.1 ppm at an air velocity of ~ 30 ft/s and gas flow rate of 2.5 SCFH. Very stable combustion inside the dimple was observed at this gas injector location. Firing rates up to 5 SCFH were achieved.

Based on the results of the single-dimple experiments, extended gas nozzles were installed in all dimples. Using a narrower channel (0.375") and plate No. 4 (2" dimple diameter, 17 dimples with cylindrical rings), very stable combustion for all dimples was achieved, with no significant interaction between dimples. Results of the emission test with all dimples fired showed O_2 – 19%, CO – 130 ppm, CO_2 – 0.1% THC – 60 ppm, NO_x – 2 ppm at ~ 1.5 SCFH gas flow rate for each dimple and ~ 15 ft/s air velocity.

In order to reach minimal possible excess oxygen in the combustion products (to increase operating temperature and efficiency), various combinations of the above-described approaches were studied. Using extended nozzles made it possible to reach 3-4% oxygen at high firing rates (~ 4 SCFH of gas per dimple). But, in this case, total hydrocarbons went up significantly (> 20,000 ppm), and complete combustion was not achieved. Combustion in only the first two or three rows of dimples resulted in ~ 3% oxygen, but only with high total hydrocarbons (> 1000 ppm).

The best single-dimple combustion results were established with dimple plate No. 4 with deep dimples (hemispherical dimples with ring), using a 3-hole natural gas nozzle inside the downstream edge of the dimple. In this case, there was 4% of oxygen in the exhaust at an air flow rate of 70 SCFH and natural gas flow rate of 6 SCFH. Total hydrocarbon concentration was 2000-5000 ppm. CO was about 2500 ppm. For the other cases, the total hydrocarbons exceeded 5000 ppm.

A variety of small tests were conducted to evaluate the effect of test channel height and gas nozzle geometry on the stability of combustion as well as its completeness in the dimples. No essential influence of channel height on dimple combustion stability or completeness was found during the tests. One of the main reasons to use a narrower channel was to decrease excess air by decreasing amount of external incoming air that is not used in combustion.

The effect of gas nozzle geometry and position on combustion stability and completeness of combustion was much more significant. Nozzles with different shapes of gas orifices, namely, slot and circular orifices, with different diameters were tested. The number of slots in the nozzle was changed from 1 to 2 and circular holes (from 1 to 3) as well as diameter of the holes (0.01-0.1").

Analysis of the experimental results showed that the smaller diameter orifices provided more stable and complete combustion because smaller orifices led to higher gas velocity and better air-gas mixing inside the dimple. Increasing the number of orifices also led to better air-gas mixing inside the dimple and more stable and complete combustion.

FOD Concept Evaluation

Experimental rig modification. A commercially available ribbon burner (Flynn Burner Corporation T-534) was selected for the laboratory concept evaluation (Figure 22).

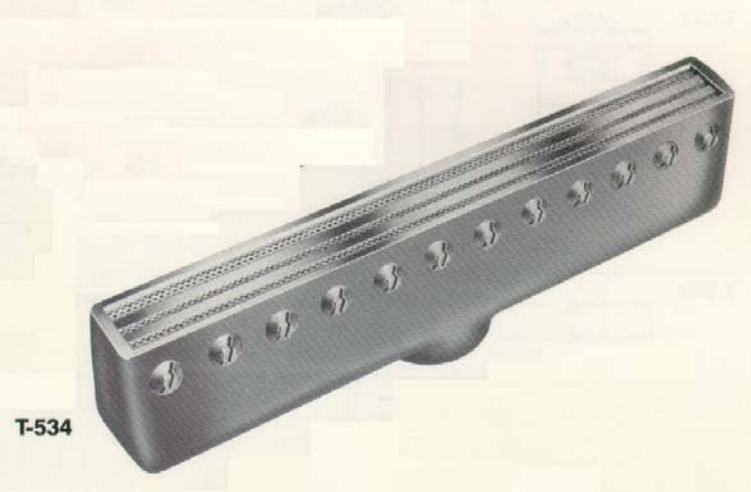

Figure 22. Three-Slot Burner T-534

The burner was installed in the bench-scale unit test section (Figure 3), and its operating envelope was determined by varying the firing rate and excess air. Figure 23 presents the measured operating envelope and Figure 24 presents a modified experimental rig.

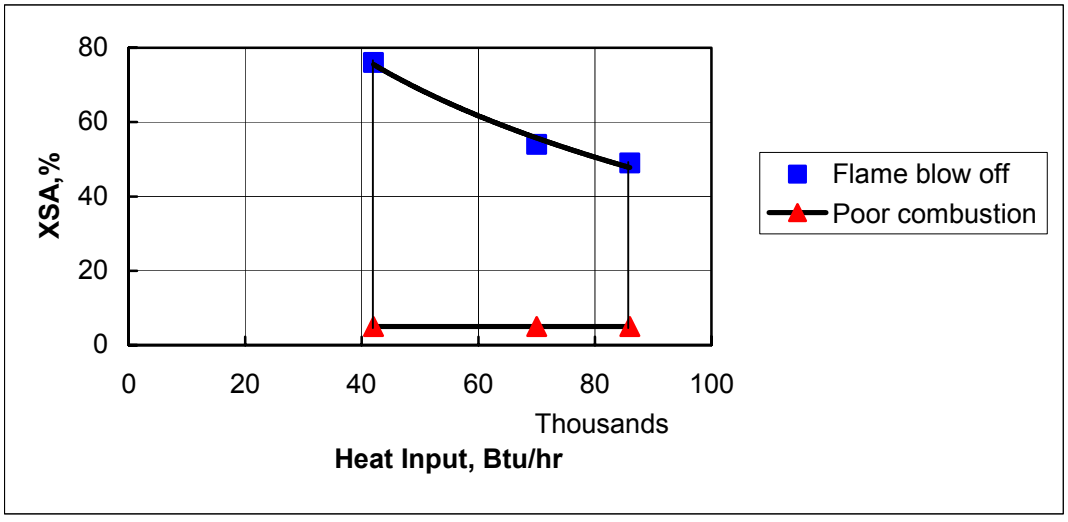

Figure 23. Operating Envelope for T-534 Installed at BSU Test Section

The burner can be stationary, installed inside a paper dryer drum, and produce a flame sheet (see Figure 2). It is also desirable to have a recirculating flow of hot flue gases to improve combustion stability and reduce flame temperature and NO_x formation. In order to simulate

recirculating flow and estimate the influence of the recirculating flow on the combustion process, cocurrent flow of hot nitrogen (as inert gas) was introduced into the test section. A nitrogen supply line was connected to the burner unit through an electrical heater to preheat the nitrogen. The supply line was insulated to minimize heat losses between the heater and the burner in order to achieve maximum nitrogen preheat temperature (up to 800ºF).

Figure 24. Modified Rig with Nitrogen Supply System

The T-534 burner was extensively tested in the modified laboratory rig, using the flat/dimpled plates installed as one of the wall of the test section. The wall outside surface temperatures were measured in order to estimate the wall temperature uniformity. The other wall of test section was a fused quartz plate that allowed observing the flame structure during the burner firing. The test results showed that the dimpled plate does not affect combustion performance.

The firing rate was varied in the range of 40,000-85,000 Btu/hr, while excess air was varied between 5 to 75% (see stable operating envelope, Figure 23). The air and gas flow rates, exhaust emissions, and flue gas and wall temperatures were measured during the each firing. The visual observation and digital recording was used to capture the typical regimes.

After determining the operational envelope of the ribbon burner, several firings were conducted to evaluate the optimal combustion regimes and explore the effect of high-speed co-flow (simulating of drum rotation). Nitrogen was selected as a co-flow agent (preheat temperature was varied from 200-800ºF) since it did not affect the combustion performance due to its inertness. It affected volumetric emission numbers only. Results for ribbon burner firing with 85 SCFH of natural gas and ~ 15% excess air are shown in the table below:

Co-Flow N_2		Exhaust Emissions			
Flow	Temperature	O_2	CO	THC	NO_X
SCFH	ºF	%	vppm	vppm	vppm
0	N/A	2.9	6	0	48
240	200	1.7	5	0	28
480	200	1.3	38	0	18
960	200	1	130	0	10
960	500	1	103	8	13
240	800	1.7	8	1	32
480	800	1.3	13	1	24
960	800	1	73	2	18

The flame was stable and combustion was complete over a wide range of nitrogen co-flow (up to 960 SCFH). The only negative fact observed during high firing was a changing flame shape that could increase temperature non-uniformity across the rotating drum, but since the estimated recirculation flow rate is 10-20% of the simulated flow there will be no flame shape affect expected.

Figure 25 shows three different flame patterns realized at different firing rates and cocurrent nitrogen flow rates.

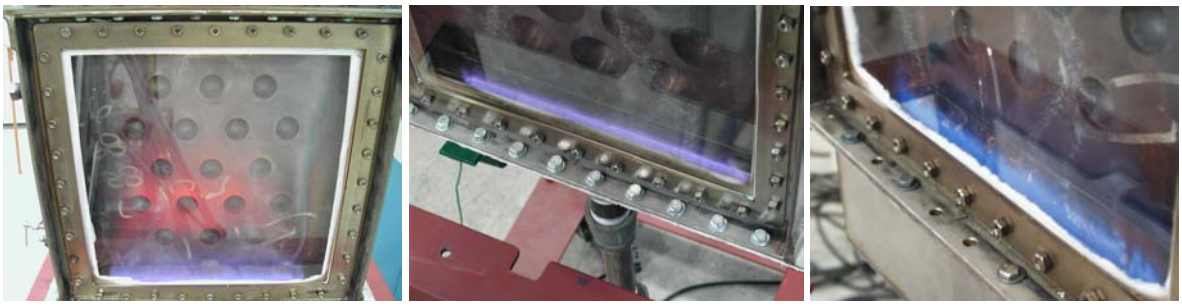

Overfiring (> 100,000 Btu/hr) | No Cocurrent Flow (~ 80,000 Btu/hr) | N_2 Cocurrent-Flow (960 SCFH) (~ 80,000 Btu/hr)

Figure 25. Snapshots of T-534 Operation

Pilot-Scale Gas-Fired Paper Dryer Development

After extensive concept evaluation, the FOD concept was selected as more promising than the FID concept for further development and testing in a pilot-scale environment. The conceptual design of the Gas-Fired Paper Dryer (GFPD) was developed and forwarded to the project partners for review, followed by engineering and fabrication.

The low-NO_x Flynn ribbon burner model T-534 was selected as a combustion device providing a high uniform sheet flow of combustion products parallel to the drum surface. GTI's innovative VHTE™ (Vortex Heat Transfer Enhancement) technology was employed in order to enhance heat transfer from the combustion products to the rotating drum and paper web.

A special deflector guide (Figure 26) provided a partial recirculation of the combustion products back to the flame root to improve combustion stability and reduce NO_X emissions.

Waste heat recuperation was considered during the concept development in order to bring up overall thermal efficiency of the GFPD significantly. A recuperator is to be incorporated into the drum design in order to provide efficient heat recovery from the exhaust gases.

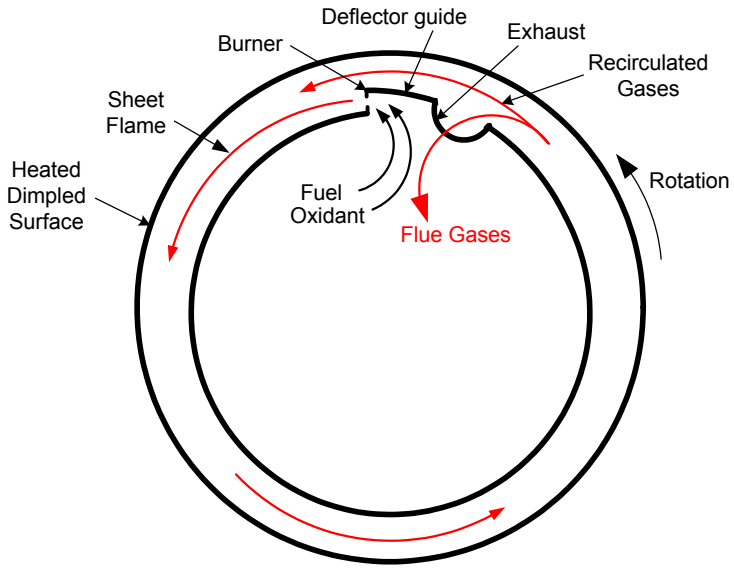

Figure 26. Final GFPD Concept

DEVELOPMENT TESTING (Phase II)

GFPD Design and Engineering

The pilot-scale unit was designed and engineered with strong support of the industrial partners. The pilot-scale GFPD was comprised of a stationary combustion system (including the burner, ignition/flame safety, and recuperator) and a rotating shell (Figure 27). All the following features were reflected in the GFPD design: flame sheet, heat transfer enhancement, partial internal recirculation of combustion products, and flue gas recuperation. Insulation was put in the exhaust of the paper drum (see Figure 27) in order to decrease heat transfer from the recirculating gases to the flue gases. The GFPD sides were also insulated to minimize the heat losses, and two view ports were placed on the side to observe the flame. A coaxial mixture supply and exhaust line work as a recuperator to transfer heat from the flue gases to the air/gas mixture.

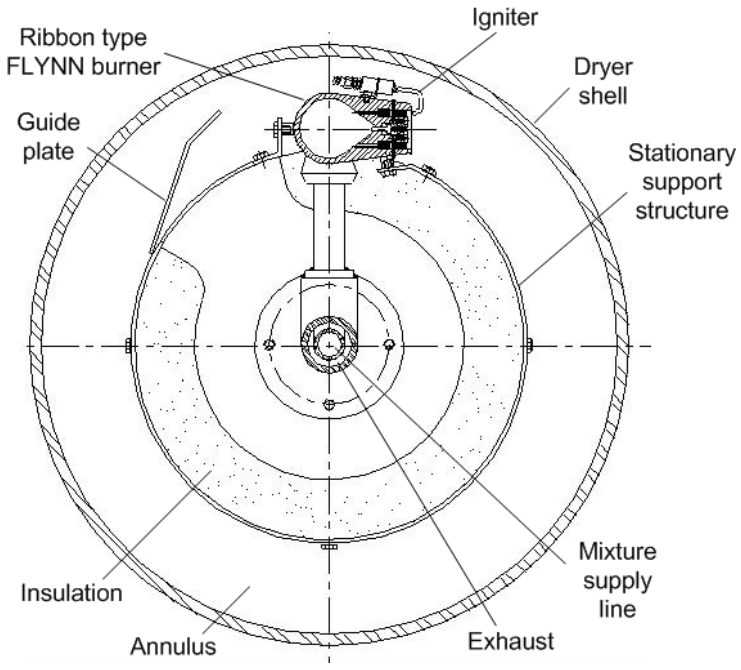

Figure 27. Pilot-Scale GFPD Design (Cross-Section of the Dryer Drum)

The ribbon burner was mounted inside the dryer on a stationary support structure that was insulated to separate the heating zone from the recuperation zone of the dryer. The rotating outer shell was profiled inside with a dimpled pattern to enhance heat transfer from the combustion products to the rotating shell. A guide plate was installed behind the burner to direct recirculated flue gases back to the root of the flame. Approximately 25% of the flue gas flow was to be re-circulated. Dimensions of the annulus, mixture supply line, and exhaust pipe, as well as the geometry of the guide plate were calculated based on hydraulic design and losses.

GFPD Laboratory Simulation

The GFPD outer drum and most of the internals were manufactured and assembled by GL&V USA Inc. with strong GTI support. Figure 28 shows the outer drum with and its dimpled inner surface. Figure 29 shows the GFPD internals along with the Flynn ribbon burner installed.

Figure 28. GFPD Outer Shell With a View of the Inner Dimpled Surface

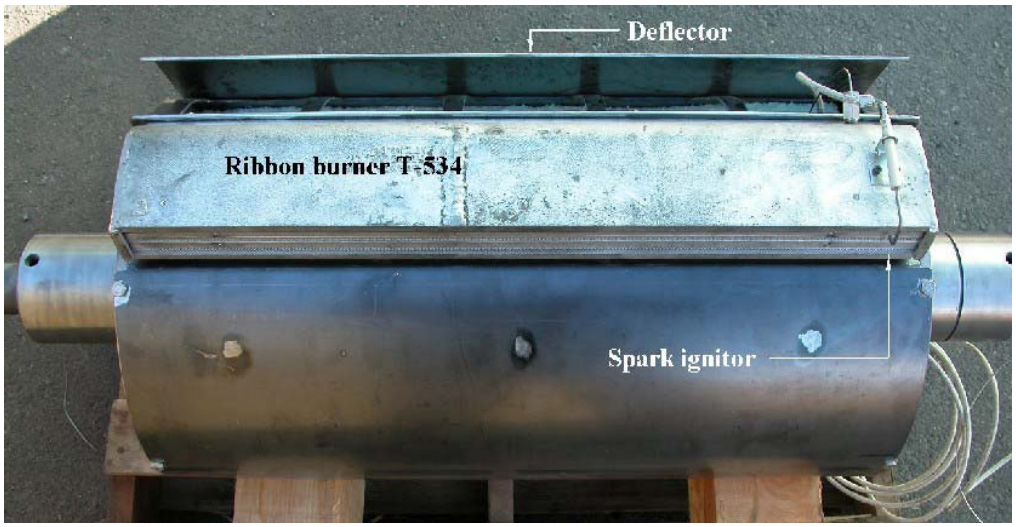

Figure 29. GFPD Combustion System

An in-house simulation of paper drying was conducted at GTI's Applied Combustion Research Laboratory to work out the combustion system prior the field installation at the WMU Paper Pilot Plant and to determine the operating envelope of GFPD. Figure 30 is a P&ID of the simulation rig, while Figure 31 illustrates it's the rig's overall layout.

During the in-house evaluation, the GFPD was fired over the range of 20,000-150,000 Btu/hr with controllable surface cooling by a wet fabric covering about 1/3 of the drum surface. The combustion system demonstrated reliable and stable operation throughout the entire test range.

The pilot-scale test procedure (including cold start up) was determined, and a drum surface temperature of 500ºF was achieved at the maximum firing rate.

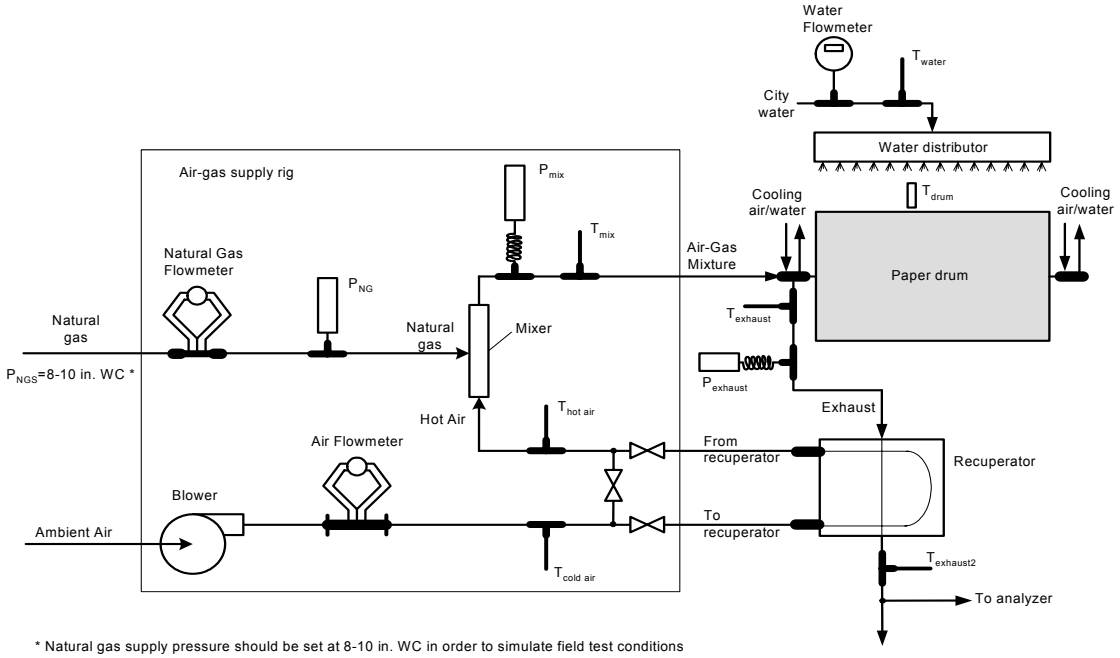

Figure 30. Piping and Instrumentation Diagram for GFPD Laboratory Simulation Rig

Figure 31. The GFPD Test Rig Equipped with Air/Gas Supply and Heat Recuperation

WMU Paper Pilot Plant

The primary objective of the testing performed at WMU Paper Pilot Plant was to provide experimental confirmation of the technical and economic feasibility of the developed natural gas-fired drum paper dryer concept in a near-industrial environment.

The Paper Pilot Plant (PPP) at WMU's Department of Paper and Printing Science (www.wmupaper.com) was selected as a test site for both baseline (conventional steam-heated) and retrofit (natural gas-fired) testing under this project. The WMU PPP offers unique capabilities in various areas of papermaking and has full-time technical personnel with extensive experience in maintenance and operation of the papermaking equipment.

The heart of the WMU PPP is a Fourdrinier paper machine that is capable of manufacturing a wide variety of papers and boards 23 inches wide at speeds up to 150 ft/min. It can manufacture paper ranging from 16 to 400 lbs basis weight. Facilities for stock and additive preparation are sized to enable continuous operation at production rates up to 160 lbs/hr.

The paper machine (Figure 32) has two independently controlled drying sections (13 drum dryers total) and is equipped with machine calendar, pope reel, and Accuray 1190 computer system with automatic basic weight and moisture control.

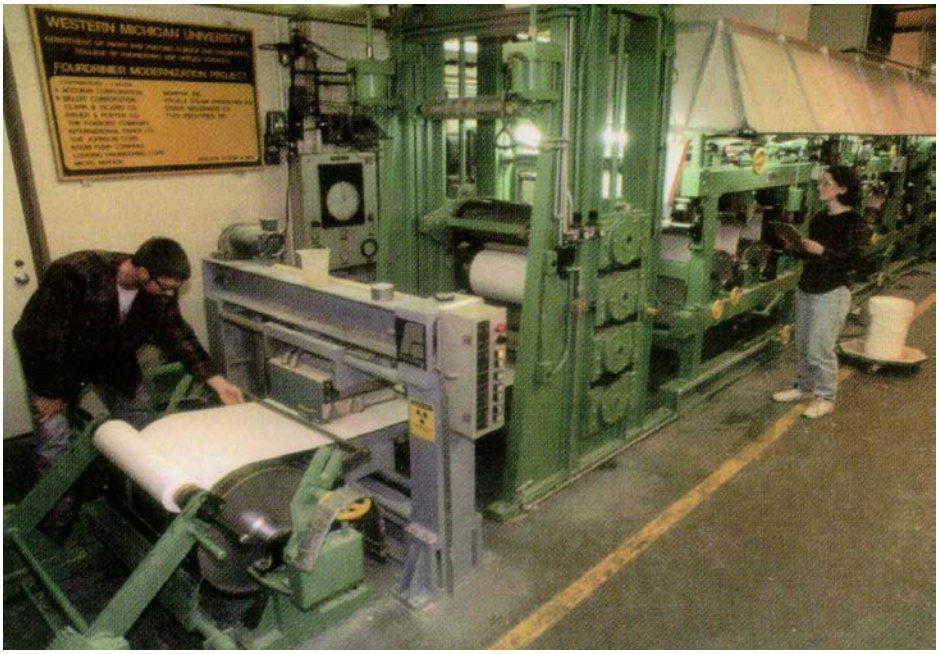

Figure 32. General View of WMU Pilot-Scale Paper Machine

Measuring System for the Testing at the WMU Facility

The measuring system was incorporated into the existing drying section layout, as shown in Figure 33. The steam supply lines were equipped with ABB steam flow meters, pressure transmitters, and control valves to measure and analyze the heat balance in the drying sections during the baseline and pilot-scale test runs. Mini-IR temperature sensors were installed above the specific test ~~steam~~ drum (#3 or #7) to measure paper inlet and outlet temperature as well

as drum surface temperature across the drum length. Two Aqua Moisture sensors were installed to measure the paper moisture content prior to and after the test drum. In order to fit the moisture sensors into the existing drying train, the inlet sensor was equipped with a low-profile IR attachment. Steam header pressures and temperatures were measured at the inlet of drums #1,2,6,8,9, and 13.

During the baseline test, the header pressures and temperatures were also measured at the inlet of drums #3 and #7. The temperature of condensate leaving the test steam drum (#3 or #7) was measured by a K-type thermocouple in order to evaluate the heat losses of the steam-heated can.

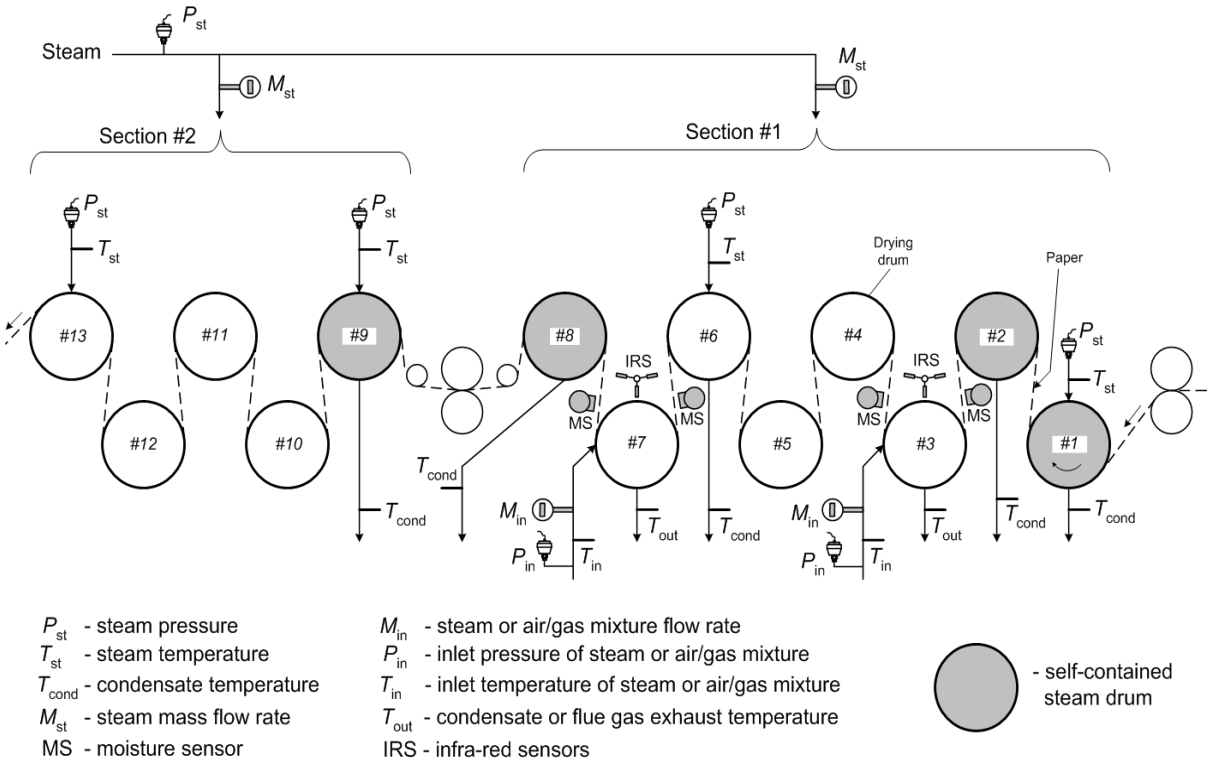

Figure 33. Measuring System Layout

During the pilot-scale test, the air/gas mixture flow rate, inlet pressure, inlet temperature, and flue gas exhaust temperature were measured at drums #3 or #7 (depending on the GFPD position). If the GFPD was installed in position #3, steam and condensate parameters were measured at drum #7 and vice versa.

All the sensors were connected to the FieldPoint data acquisition system. The data were real-time monitored and recorded using National Instruments' LabView software on a laptop computer.

The following parameters were measured during baseline testing:

• **Pressure:**	• **Flow rate:**
- Steam supply lines	- Steam supply for 1st section
- Steam inlet of drums 1,3,6,7,9,13	- Steam supply for 2nd section
	- Steam supply for test drum
• **Temperature:**	• **Moisture:**
-Steam inlet of drums 1,3,6,7,9,13	- Paper web before/after test drum
-Steam condensate at drum 1,2,3,7,8,9	
-Paper between each drum (manual)	• **Machine Parameters:**
-Surface of the test drum (IR)	-Stock flow
-Paper web before/after test drum (IR)	-Machine speed
-Surface of all drums (manual)	-Dry end moisture
-Paper between each drum (manual)	-Basis Weight

Exhaust gas composition (O_2, CO, CO_2, NO_X) was measured by a portable Horiba PG-250 gas analyzer and recorded using National Instruments' LabView data acquisition system on another laptop computer.

Paper samples were taken before and after each dryer to evaluate the paper physical properties such as basis weight, burst, caliper, Gurley stiffness, elongation, tear, and tensile strength.

Data Processing Approach

Based on the measured parameters, the paper drying rate and drying efficiency were calculated. The drying rate (R_w) is defined by TAPPI method (TIP 0404-07) as the amount of water evaporated per hour per unit of drying surface. Drying surface is defined as the total circumferential length of the steam-heated dryers multiplied by the width of the sheet at the reel. The following equations are used to calculate the drying rate:

$$M = L/E\text{-}1 \text{ and } R_w = 60SBM/(NA\pi D), \text{ lb water evaporated /hr/ft}^2,$$

where the factor 60 is minutes per hour and the variables are defined as:

R_w = drying rate, amount of water evaporated, lb/(hr*ft^2)

S = machine speed, ft/min

B = basis weight of the sheet as it leaves the dryer section as dried (wet basis), lb/ream

M = weight of water evaporated per unit weight of paper as dried (wet basis)

N = number of steam-heated dryers that contact the sheet

A = area of standard ream (3000 ft^2)

π = 3.1416

D = diameter of dryer cylinders, ft

L = percent dryness (wet basis) of sheet leaving the last cylinder (larger number) (Percent dryness = 100% – percent of moisture content in the paper.)

E = percent dryness (wet basis) of sheet entering the first cylinder (smaller number)

The drying efficiency (*Eff*) is calculated as the ratio between the heat needed for water evaporation and the heat input from steam or natural gas:

$$Eff = Q_{evap} / Q_{in}.$$

Heat needed for water evaporation is calculated as the product of the amount of moisture evaporated per hour (W) and the specific enthalpy of the steam (E_{st}):

$$Q_{evap} = W * E_{st}\text{, Btu/hr}$$

The heat input from steam is calculated as the product of the steam mass flow rate (M_{steam}) and the specific enthalpy of steam:

$$Q_{in} = M_{steam} * E_{st}\text{, Btu/hr}$$

The heat input from natural gas is calculated as:

$$Q_{in} = Q_{mix} + Q_{comb} - Q_{ex}\text{, Btu/hr}$$

Where Q_{mix} is the air-gas mixture heat flow calculated as:

$$Q_{mix} = M_{mix} (c_p)_{mix} T_{mix}\text{, Btu/hr}$$

Q_{comb} is the heat flow from combustion calculated as:

$$Q_{comb} = M_{NG} G\text{, Btu/hr}$$

Q_{ex} is the flue gas heat through the exhaust calculated as:

$$Q_{ex} = M_{mix} (c_p)_{FG} T_{FG}\text{, Btu/hr,}$$

where:

M_{mix} = mixture mass flow rate (lb/hr)

M_{NG} = natural gas volume flow rate (SCFH)

$(c_p)_{mix}$ = mixture specific heat at inlet temperature (Btu/lb/ºF)

$(c_p)_{FG}$ = flue gas specific heat at exhaust temperature (Btu/lb/ºF)

T_{mix} = mixture inlet temperature (ºF)

T_{FG} = gas temperature at exhaust (ºF)

G = natural gas gross heating value (Btu/SCF)

Basis weight is defined by TAPPI method T-410 in lbs per ream (or g/m^2). Bursting strength is defined by TAPPI method T-403 as the hydrostatic pressure in pounds per square inch (or kPa), required to produce rupture of the material when the pressure is increased at a controlled constant rate through a rubber diaphragm to a circular area 1.2-inch diameter. Thickness or

caliper of paper as measured by TAPPI method T-441 and is defined as the perpendicular distance between the two principal surfaces of the paper under prescribed conditions. Gurley stiffness is defined as the bending moment in pound-inches required to bend a clamped strip of paper through a specified angle (TAPPI method T-543). Internal tearing resistance of paper is defined by TAPPI method T-414 as the force perpendicular to the plane of the paper required to tear a sheet of paper. Tensile strength is defined by TAPPI method T-494 as the maximum tensile stress developed in a test specimen before rupture on a tensile test carried to rupture under prescribed conditions. Tensile strength is force per unit width of the test specimen (kN/m). The stretch (or percentage elongation) is defined by TAPPI method T-494 as the maximum tensile strain developed in the test specimen before rupture in a tensile test carried to rupture under prescribed conditions. The percentage elongation is expressed as a percentage, i.e., one hundred times the ratio of the increase in length of the test specimen to the original test length.

Baseline Tests at WMU Paper Pilot Plant

Description of Tests

Steam drums 3 and 7 were selected for baseline evaluation (Figure 34). Drum #3 was selected per WMU recommendation as the most thermally loaded drum in the drying section. Drum #7 was selected for evaluation of GFPD performance at lower inlet paper moisture levels. The baseline test plan was to measure drum surface temperatures and paper moisture profiles across the paper web at maximum heat input levels (maximum steam flow at the drums #3 and #7).

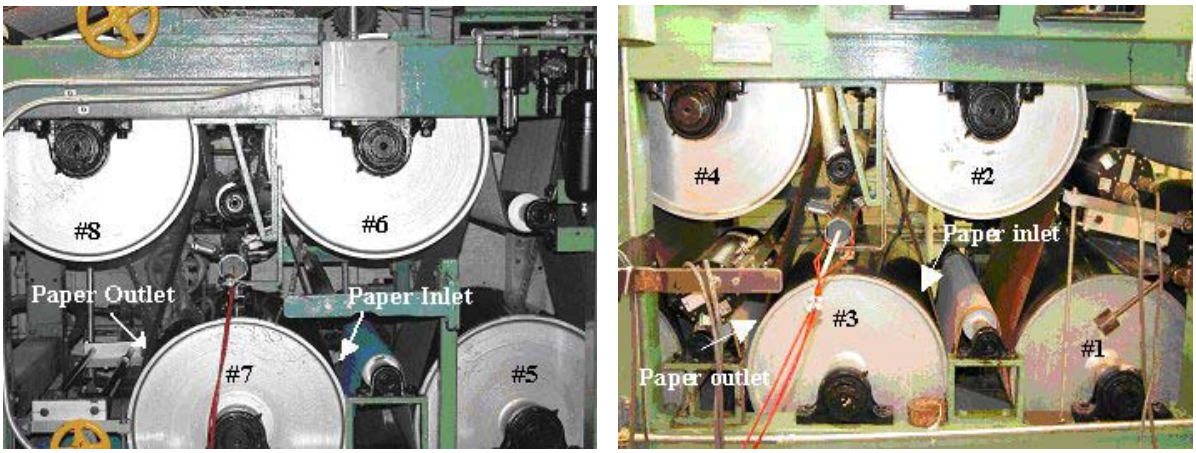

Figure 34. Steam drums #3 and #7 instrumented for baseline test

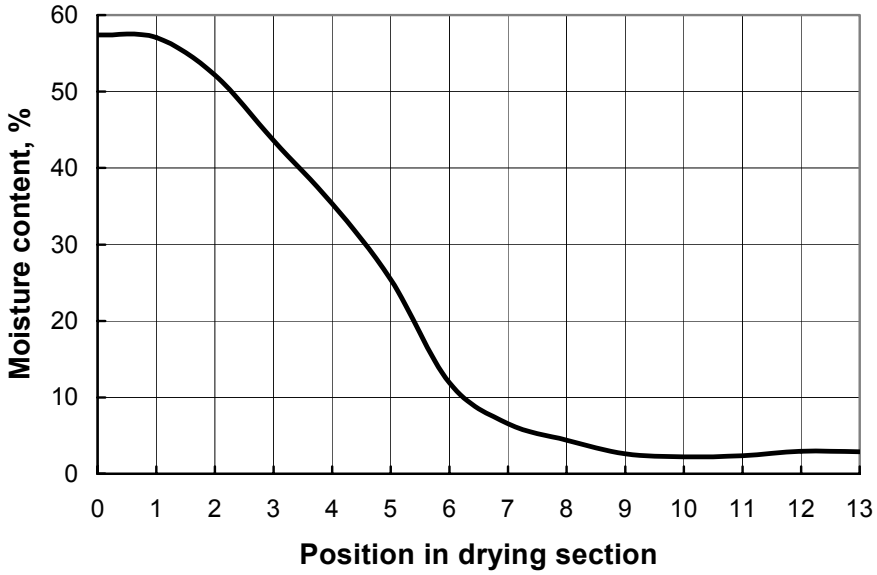

Figure 35. Typical Paper Moisture Distribution Through the WMU Pilot-Scale Paper Machine
(Four sets of paper samples were taken at the inlet and outlet of each drum for averaging.)

The paper moisture level at the inlet of the test drums was kept relatively constant in the target ranges of 10%-60% (Constant Drying Rate Zone, see Figure 35) for all baseline runs (see Table 2). Steam was supplied separately to the main drying section (drums #1-8) and the after drying section (drums #9-13). Changing the steam header pressure in these sections allowed active control of the steam flow through the drums and the paper moisture levels and drying rates along the drying train. At the highest paper moisture level (60%), the steam flow to the test drums was varied to evaluate the effect of heat flow on drying efficiency. The highest drying efficiencies were achieved at the highest heat flow levels; therefore, this test was not conducted at low moisture levels.

Table 2: Matrix of WMU Baseline Testing

Inlet Paper Moisture (%)	Maximum Heat Flow (Btu/Hr)	Dryer Position #
10	60,000	7
20	60,000	7
30	60,000	7
60	90,000	3
60	35,000	3
60	0	3

Baseline Test Results

According to the baseline test plan matrix, all data were collected, processed, and analyzed. Table 3 illustrates the paper machine operating parameters. These data represent the overall ranges of values at baseline conditions along with the corresponding value of maximum deviation for any particular test.

One of the most important factors in paper drying is temperature uniformity across the drum dryer. Figure 36 shows time-averaged temperature distribution (surface, paper inlet and paper outlet) across the drum at the maximum heat input of 90,000 Btu/hr.

Drying rates and drum efficiencies were calculated for the steam-heated dryers. Table 4 displays the dryer performance (results are presented for three different machine settings).

The values in Table 4 represent an inlet paper moisture content ranging from 52% to 55% for drum #3 and from 12% to 30% for drum #7. It should be noted that drying rate and efficiency depend on many parameters including heat input, drum surface temperature, and inlet moisture content.

Table 3: Baseline Test Operating Parameters

Total heat flow: 620,000 - 700,000 Btu/hr
Heat flow through the test drum: 0 – 90,000 Btu/hr
M_{in} = 11-58% (maximum deviation - 3%)
$(T_{paper})_{in}$ = 114-178ºF (maximum deviation - 3.7ºF)
T_{drum} = 126-251ºF (maximum deviation - 12ºF)
$(T_{paper})_{out}$ = 104-173ºF (maximum deviation - 10ºF)
Steam Pressure Main Section = 10-21 (psi)
Steam Pressure Aft Section = 3-10 (psi)
Steam Temperature = 190-260 (°F)
Machine Speed = 28.0 – 28.8 (fpm)
Paper Width (inlet) = 23.375-26.125 (inches)
Paper Width (outlet) = 22.5-25.375 (inches)
Basis Weight = 97.3-129.4 (lb/ream)

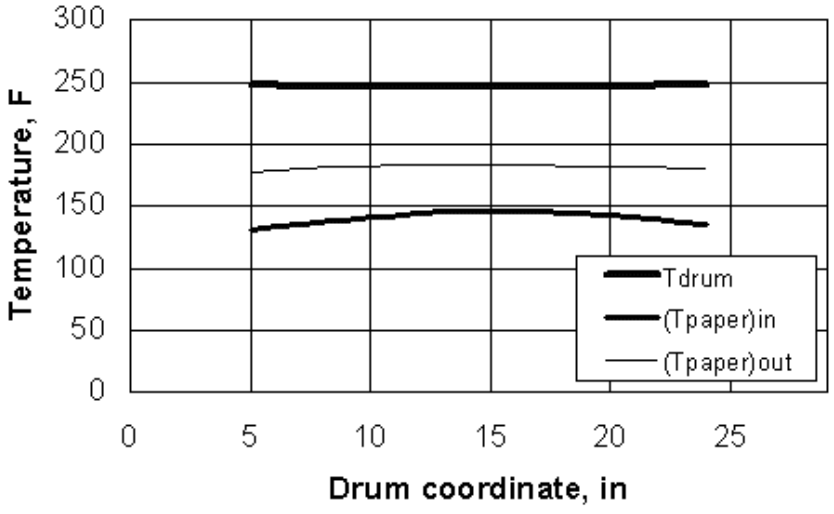

Figure 36. Paper, Pre/Post Drum (#3) Temperatures at Different Axial Positions (55% Inlet Moisture)

Table 4: Drying Rate and Efficiency Results for Steam Drums

Dryer Location	Steam flow rate, lb/hr	Steam temp., ºF	Drum temp., ºF	Inlet moisture content, %	Moisture removal, %	Drying rate lb/(hr*ft^2)	Drying efficiency, %
Test #1 (baseline)							
Entire Machine	642	235	229	57	54.6	1.3	27
Steam dryer #3	98	259	249	52	8.5	2.4	43
Steam dryer #7	49.7	260	252	12	5.3	0.8	17
Test #3 (baseline)							
Entire Machine	653	231	222	57	54.2	1.4	32
Steam dryer #3	76	237	228	55	5.0	1.5	44
Steam dryer #7	42.3	237.8	230	30	3.9	0.8	27
Test #4 (baseline)							
Entire Machine	706	239	232	57	54.4	1.3	28
Steam dryer #3	94	257	247	54	6.5	1.9	45
Steam dryer #7	51.5	258.1	251	21	10.8	1.9	45

GFPD Testing at Elevated Temperature

During the pilot-scale test the GFPD drum was installed in the drum #3 position (Figures 33 and 37) to test it at inlet paper moisture levels around 55% (wet end) and in the drum #7 position to evaluate the GFPD performance at inlet paper moisture levels of 10%-40% (dry end). The instrumentation of the paper machine for the GFPD test was the same as during the baseline test, with the exception of steam-measurements at drums #3 and #7. Figure 37 shows the GFPD during firing. An advanced air/gas flow management and mixing system, equipped with high accuracy vortex flow meters and portable gas analyzer, was used to control and monitor flame stoichiometry and exhaust emissions.

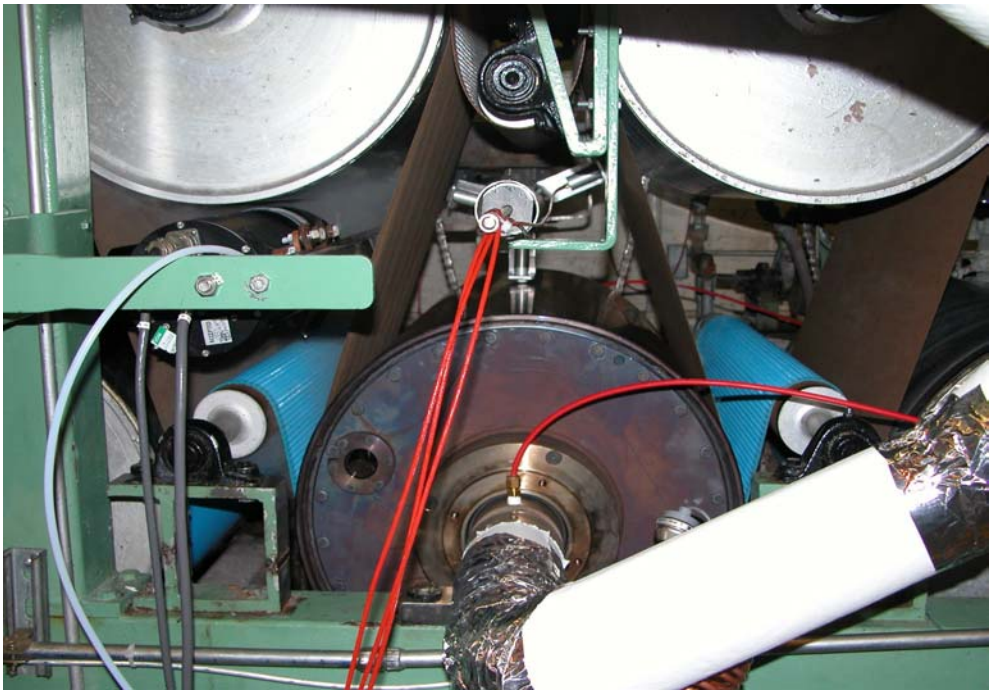

Figure 37. GFPD Layout

Typical paper moisture content distribution through the paper-drying machine with GFPD installed at position #7 is shown in Figure 38.

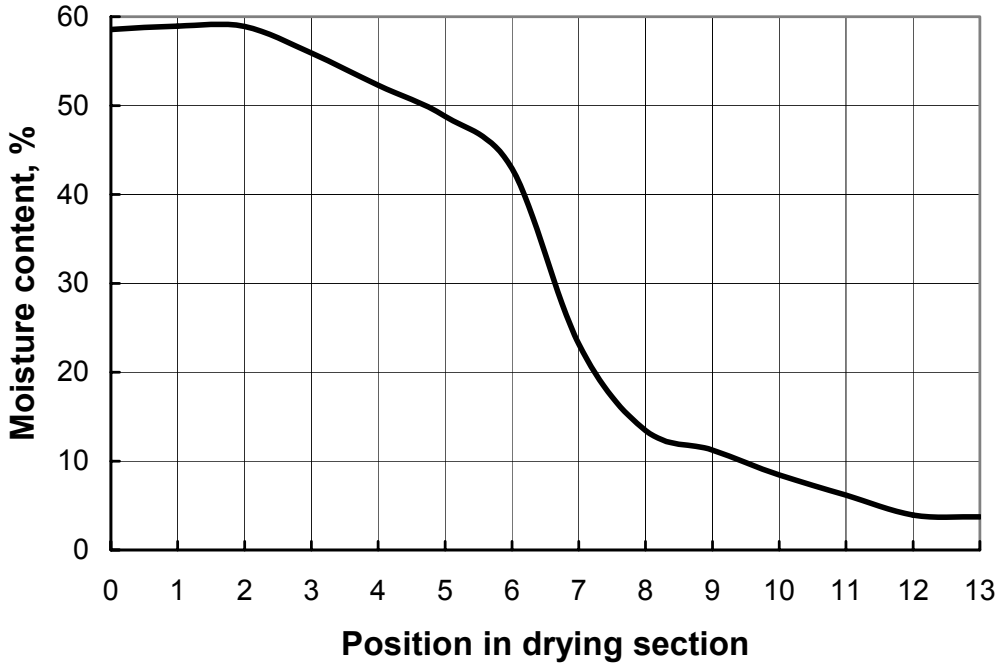

Figure 38. Paper Moisture Through the Drying Machine with GFPD Installed at Position #7
(Four sets of paper samples were taken for averaging.)

GFPD Drum Surface Temperature

In order to vary the test drum surface temperatures, the burner was fired at rates ranging from 17,000 to 130,000 Btu/hr (see Figure 39). The average drum surface temperatures ranged from 264°F to 467°F, with a standard deviation ranging from ±3%-±9%. The highest average drum surface temperature was 467°F with a standard deviation of ±17°F. The GFPD surface temperature was limited to 500ºF due to the operating limit of the high-temperature felt used to press the paper to the drum (monofilament fabric Kleenflex 69, donated to the project by Albany International Company).

Radial Burner Position

The design of the GFPD allows the burner to be positioned at any angle around the drum circumference by rotating the entire support structure. It was visually observed that a vertical position of the ribbon burner had the largest effect on flue gas recirculation. It was also observed the flame curved around the top of the burner and reversed its direction at several test conditions (Figure 40). As firing rate was increased to 50,000 Btu/hr, the flame returned to the fire-forward direction. An increased burner mixture temperature also produced this effect, since, in case of flame reversal, the flame was not separated from the burner and stayed attached to the top of the burner causing excess heating of the burner. This phenomenon did not occur at the -90° position (see Figure 41).

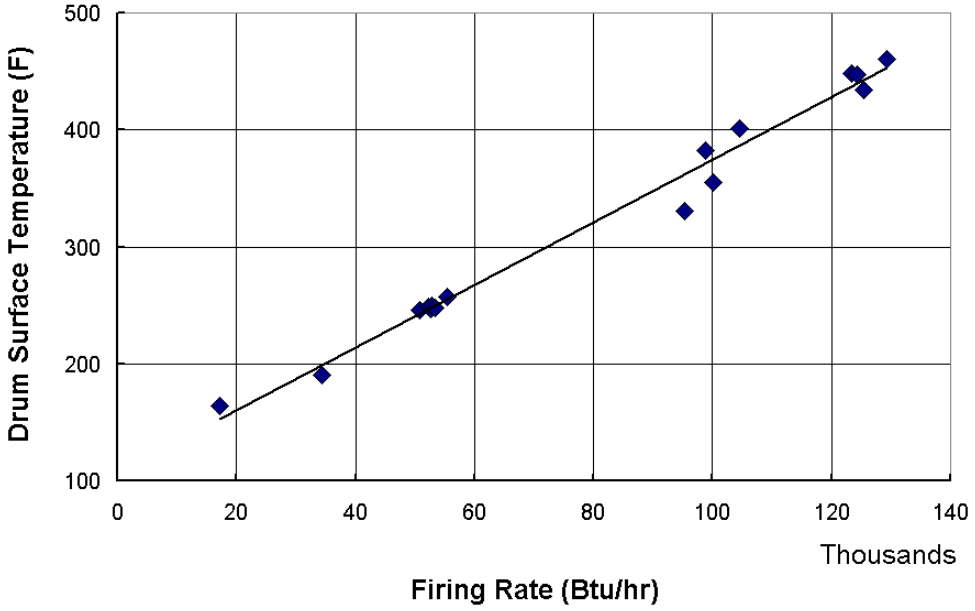

Figure 39. GFPD Surface Temperature vs. Firing Rate at 55% Inlet Moisture at Drum Position #3

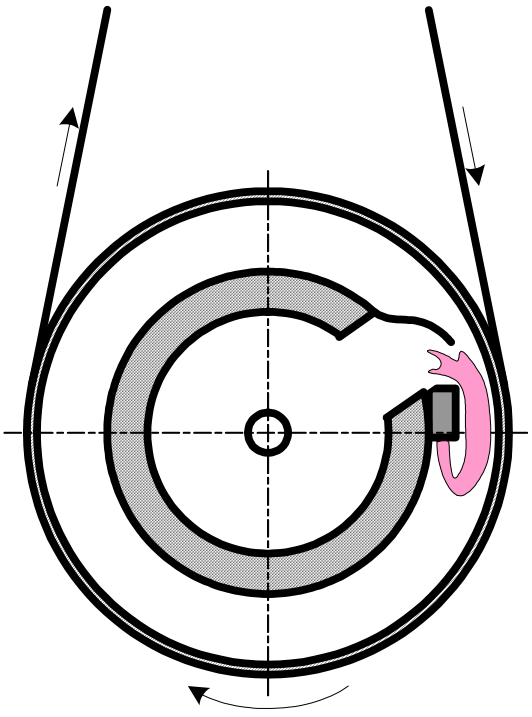

Figure 40. Flame Curved Around the Top of the Burner

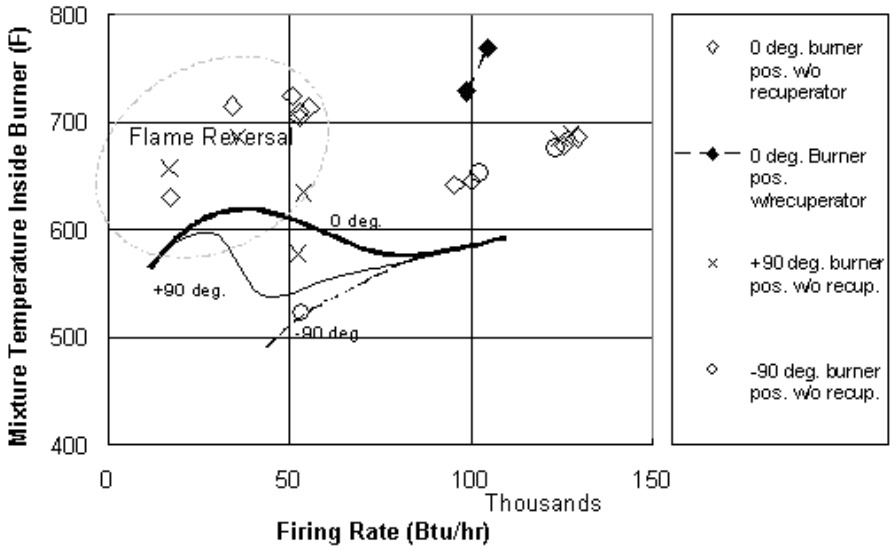

Figure 41. Gas-Air Mixture Temperature vs. Firing Rate at 55% Inlet Moisture

Drying Rate and Efficiency

The GFPD increased drying rate in about 4-5 times over the average value measured for steam heated drum (Figure 42). Drying efficiency was also calculated for the corresponding GFPD drying rates. Figure 43 illustrates the dependence of drying efficiency on natural gas firing rate for data taken at the wet end (drum #3). At the highest firing rate of 130,000 Btu/hr, drying efficiencies of about 60% were achieved at paper inlet moisture levels of 55%, while maximum drying efficiency for a steam drum was estimated as 45%. It is known that the maximum overall efficiency of a steam dryer can be projected as 68% (assuming 15% losses in the boiler, 10% in the transmission system, and 10% in the dryer can).

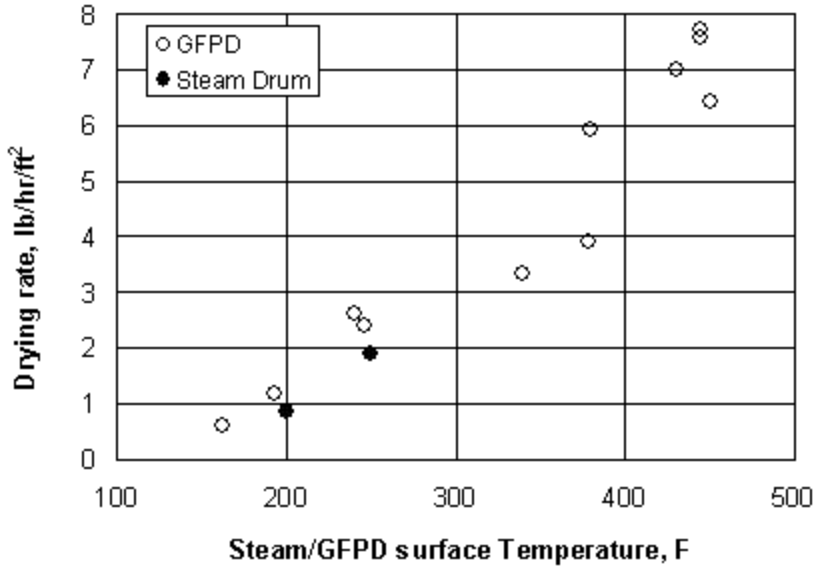

Figure 42. Drying Rate vs. Drum Surface Temperature at 55% Inlet Moisture

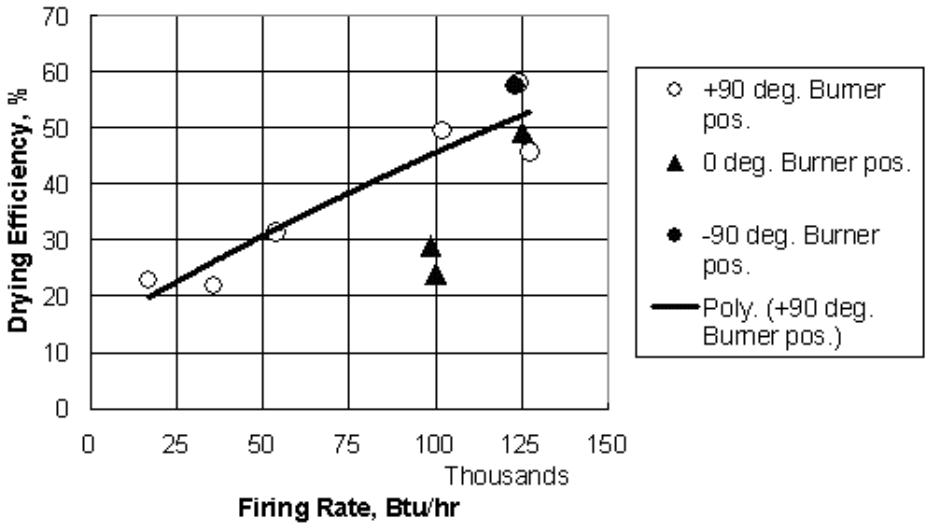

Figure 43. Drying Efficiency vs. Firing Rate at 55% Inlet Moisture

On the dry end (drum #7), a maximum efficiency of 71% was achieved, with a corresponding drying rate of 4.9 lb/hr-ft^2, at a surface temperature of 430ºF and an inlet paper moisture level of 43% (see Table 5). It should be noted that, at higher firing rates, (>130,000 Btu/hr) much higher efficiency would be achievable.

Table 5: Results for Representative GFPD Tests on the Dry End

Dryer Location	Steam/Gas flow rate	Steam/Gas inlet temp.	Drum temp.	Inlet moisture content	Moisture removal	Drying rate	Drying efficiency**
	lb/hr	ºF	ºF	%	%	lb/(hr*ft2)	%
Test #1							
Entire Machine	476.9	220	199	58	54.5	1.4	39***
GFPD (dryer #7)	2.7	154	279	41	5.7	1.3	51
Test #2							
Entire Machine	463.2	220	204	57	54.2	1.4	38***
GFPD (dryer #7)	4.4	164	352	38	11.0	2.4	51
Test #3							
Entire Machine	378.5	213	204	59	54.8	1.4	44***
GFPD (dryer #7)	6.4	165	430	43	19.7	4.9	71

** Based on average of 4 paper samples*
***Calculated based on heat needed for water evaporation and heat input from steam and combustion*
**** Taking into account heat input from steam and natural gas combustion*

GFPD Emissions

Natural gas emissions produced by GFPD were constantly monitored during the testing and were all found to be within acceptable limits. Air/gas ratio was controlled to allow 2-3 % O_2

in the exhaust products. Table 6 displays the exhaust emissions measured at the maximum firing rate of 130,000 Btu/hr.

Table 6: Exhaust Emissions Ranges for All GFPD Tests (Corrected to 3% O_2)

Species	Range
NO_x	30-114 (vppm)
CO_2	10.2-11 (%)
CO	3-30 (vppm)

Paper Quality

Several paper strength properties were measured in order to determine the effect of higher temperature drying on paper quality. The paper quality analysis was performed by the WMU Paper Quality Laboratory and the results are presented in Table 7. The data for the baseline and GFPD tests were based on averaging of 10 test samples. Table 7 demonstrates no tangible difference in the paper strength properties between baseline and GFPD tests, which were carried out at very different temperatures.

Table 7: Strength Properties of the Paper (Linerboard)

	Drum #7 Surface Temperature, ºF	Basis Weight, g/m^2	Bursting strength, kPa	Caliper, 1/1000 in.	Gurley stiffness, GF units	Elongation, %	Tearing resistance, gf	Tensile strength, kN/m
Baseline Test	238	213	323	14.8	3.9	1.7	240	7.0
GFPD Test	430	210	351	15.0	4.5	1.8	233	7.9

CONCLUSIONS

The results of GFPD testing at the WMU Paper Pilot Plant successfully demonstrated the advantages of a natural gas-fired approach while producing an industrial linerboard (126 lb/3000 ft^2). It was proven that drum dryer surface temperature could be increased up to 500-600ºF. High-temperature operation results in significant improvement in drying rate and efficiency over conventional steam-heated drums without sacrificing product quality.

The GTI pilot-scale tests at WMU showed that the maximum drying efficiency for the GFPD (calculated as the ratio of heat required for evaporation/heat released by natural gas) is 75% compared to the 55% maximum drying efficiency (calculated as the ratio of heat required for evaporation/heat from steam condensation) for the comparable steam-heated dryer. Overall efficiency of the GFPD (calculated as the ratio of Useful Heat/Total Heat Input) could be boosted up to 85% through internal flue gas recuperation (for example, combustion air

preheat). The maximum value of the steam dryer overall efficiency can be projected as 68% (assuming 15% losses in the boiler, 10% in the transmission system and 10% in the dryer can).

The TAPPI drying rate achieved with gas-fired operation was 4-5 times higher than with conventional steam operation. This was due to operating at a higher drum temperatures (the GFPD test was restricted by a felt temperature limit of 450ºF). Figure 42 illustrates the GFPD results on WMU's Fourdrinier pilot-scale paper machine for industrial linerboard production. The maximum increase in drying rate potential on full-scale paper machines will depend on actual operating conditions and paper grade and is subject to determination during GFPD field trials.

The conventional steam-heated drum at WMU consumed about 70,000 Btu/hr of saturated steam heat to reach 250ºF on the drum surface compared to the less than 50,000 Btu/hr of heat needed to reach the same surface temperature for the GFPD. Moreover, to reach 500ºF on the gas drum surface (which is not possible with steam heating) the heat input would need to be increased by only 70% over the steam heated drum (up to 120,000 Btu/hr). It is believed that the gas-fired operation could allow reaching a higher TAPPI drying rate even at the same drum surface temperature due to the absence of a condensate level on the bottom of the drying can that increases thermal resistance to the paper web.

Preliminary estimates indicate that the GFPD drying system could lead to a production increase of up to 20% without a dry end extension of the paper machine. Production rate increase will depend on drum operating temperature and number of drums installed/replaced. Even if an existing paper machine is not drying-rate limited, the GFPD may be used to reduce energy consumption.

RECOMMENDATIONS

The results of the R&D conducted to date indicate that the development of the GFPD should be continued in order to achieve that following:

- Determine the optimum number of GFPD drums in a typcal paper line and their optimal positions.
- Achieve drum surface temperature uniformity of ±5ºF.
- Increase the utilization of exhaust heat to improve efficiency. Promising approaches include combustion air preheat and pocket ventilation.
- Improve recirculation inside the drum to reduce NOx emissions and increase combustion stability.
- Reduce NO_x emissions to 20-30 vppm level.
- Ensure safety through combustion controls, flame sensing, reliable ignition, and quick cool-down to safe temperatures in the paper line stops or the paper web breaks.

ACKNOWLEDGEMENTS

The project team is grateful to U.S. Department of Energy (award DE-FC36-01GO10621), GRI (contract 8477), and Members of GTI's Sustaining Membership Program for their financial support of this work. We are also grateful to the project's industrial partners - Boise Paper Solutions (Donald Harrison), GL&V USA Inc. (Fred Elbert and Stan Green), and Flynn Burner Corporation (Joseph DiGiacomo and James Pezzuto) for their significant technical contributions to this development.